National Defence / Défense nationale

ON THE IMPLEMENTATION OF THE STRIP SPECTRAL CORRELATION ALGORITHM FOR CYCLIC SPECTRUM ESTIMATION

by

Eric April

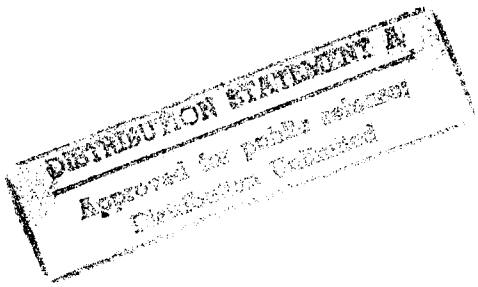

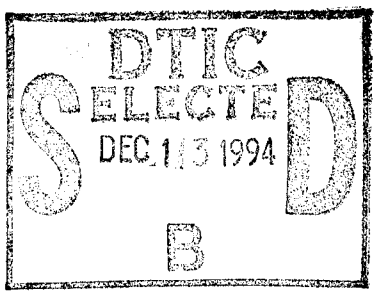

DEFENCE RESEARCH ESTABLISHMENT OTTAWA
TECHNICAL NOTE 94-2

Canada

February 1994
Ottawa

National Defence / Défense nationale

ON THE IMPLEMENTATION OF THE STRIP SPECTRAL CORRELATION ALGORITHM FOR CYCLIC SPECTRUM ESTIMATION

by

Eric April
Electronic Support Measures Section
Electronic Warfare Division

DEFENCE RESEARCH ESTABLISHMENT OTTAWA
TECHNICAL NOTE 94-2

PCN
041LK11

February 1994
Ottawa

ABSTRACT

This report discusses the implementation of one of the best digital cyclic spectrum (CS) algorithms derived so far, the Strip Spectral Correlation Algorithm (SSCA). Some theoretical background and a detailed description of the SSCA are provided. An analysis of the SSCA is performed and an algorithm for mapping the SSCA output is formulated. The cyclic feature function (CFF) is defined as a means to detect the cyclic features from the SSCA. Results of the SSCA encoded in C are then reported. Three BPSK signals and two additive white Gaussian noise (AWGN) signals are used to verify the validity of the SSCA. Three-dimensional plots and two-dimensional plots of the CS and CFF respectively are presented to the reader. Finally, some benchmarks on a SUN computer for the SSCA are provided for reference. In brief, the CS and CFF estimated with the SSCA prove to be valuable tools for analyzing second-order cyclostationary communication signals and, by making extensive use of the FFT, to provide robust, reliable, and accurate results more efficiently than typical CS direct estimation methods.

RÉSUMÉ

Ce rapport traite de la mise en oeuvre de l'un des meilleurs algorithmes élaborés à ce jours pour ce qui est de l'estimation complète du spectre cyclique (SC) d'une séquence numérique, soit l'algorithme SSCA. Les bases théoriques et la description détaillée du SSCA sont fournies. L'analyse du SSCA est effectuée et un algorithme destiné à réordonner les résultats du SSCA est formulé. La fonction de caractéristique cyclique (CFF) est définie et employée afin de détecter les caractéristiques cycliques à partir de l'algorithme SSCA. Les résultats du SSCA codé en langage C sont ensuite rapportés. Trois signaux BPSK ainsi que deux signaux composés de bruit blanc Gaussien additif sont utilisés pour vérifier la validité du SSCA. Les représentations graphiques en deux et trois dimensions respectivement du CFF et du SC sont présentées au lecteur. Finalement, des points de repères en ce qui concerne le temps d'exécution du SSCA sur un ordinateur SUN pour les paramètres utilisés sont fournis à titre de référence. En bref, le SC et le CFF estimés à l'aide du SSCA constitue assurément des outils importants pour l'analyse de signaux cyclostationnaires de deuxième ordre et, par une vaste utilisation de la FFT, le SSCA permet de produire des résultats robustes, fiables et précis de façon beaucoup plus efficace que d'autres méthodes numériques plus directes d'estimation du SC.

EXECUTIVE SUMMARY

Athough much superior to ordinary spectral analysis, cyclic spectral analysis requires considerably more complex and time-consuming computations to produce an estimate of the entire cyclic spectrum (CS). An estimate of the entire CS is required when a priori information on signal cycle frequencies is not available. In this case, detection of cycle frequencies possibly through the CS is crucial to any cyclostationary property exploiting methods for several applications encountered in typical military surveillance system such as, for example, signal detection and classification, signal's parameter estimation, time-difference of arrival estimation, adaptive spatial filtering, direction finding and signal extraction. Based on either a frequency or time-smoothing approach, efficient algorithms for estimating the cyclic spectrum of discrete-time domain signals have been devised during the last decade or so. This report discusses the implementation of one of the best digital CS estimation algorithms derived so far, the Strip Spectral Correlation Algorithm (SSCA).

Following a review on the theory of spectral correlation for cyclic spectral analysis of discrete-time signals, the SSCA is derived. The detailed description shows that the SSCA essentially reduces in complexity to a two-dimensional FFT of size NxN_p and that it is suitable for parallel architectures. Parameters N, denoting the observation time, and N_p, specifying the number of samples considered in the channelizer, determine a number of CS estimate attributes such as the frequency resolution Δf, the cycle frequency resolution $\Delta\alpha$, and the time-frequency resolution product $\Delta f \Delta t$. All the steps required to implement the SSCA are clearly explained. An analysis of the SSCA reveals its computional requirements. The accuracy of the estimates are also considered and an algorithm for mapping the SSCA output is provided. Additionally, the cyclic feature function (CFF) is defined as a means to detect the cyclic features from the SSCA. Results of the SSCA encoded in C are then reported.

Theoretical CSs are derived for three BPSK signals using various parameters and two additive white Gaussian noise (AWGN) signals. Three-dimensional plots of the CS and two-dimensional plots of the CFF of various combinations of these signals along with various algorithmic parameters are realized with the **ssca** program and presented to the reader. Specifically, the effect of varying the observation time and the frequency resolution are observed on one BPSK signal and one AWGN independently. Then, the CS and CFF of combinations of the signals under investigations are studied while keeping all SSCA parameters fixed. Cyclic features are detected based on the CFF. These experimental

results show that all major cyclic features, corresponding directly or indirectly to signal features (e.g. carrier frequency and baud rate in this case), are successfully detected even in highly corrupted conditions where conventional analysis would have failed to discriminate the signals. Finally, some bechmarks on the SUN computer for the SSCA are provided for reference.

In brief, the CS and CFF estimated with the SSCA prove to be valuable tools for analyzing second-order cyclostationary communication signals and, by making extensive use of the FFT, to provide robust, reliable, and accurate results more efficiently than typical CS direct estimation methods. This suggests further work to apply the SSCA to off-air data and possibly implement the algorithm in a popular digital signal multi-processor board such as a C40 board.

TABLE OF CONTENTS

	Page
ABSTRACT/RÉSUMÉ	iii
EXECUTIVE SUMMARY	v
TABLE OF CONTENTS	vii
LIST OF FIGURES	ix
LIST OF TABLES	xi
1.0 INTRODUCTION	1
2.0 BACKGROUND	1
2.1 Basic Frequency-smoothing Approach	2
2.2 Basic Time-smoothing Approach	3
2.3 Comments on Both Approaches	3
3.0 THE STRIP SPECTRAL CORRELATION ALGORITHM	4
3.1 From the Basic Time-smoothing Approach to the SSCA	4
3.2 SSCA Description	6
3.3 SSCA Analysis	9
3.3.1 Computational Requirements	11
3.3.2 Accuracy of the Estimates	12
3.3.3 Mapping Associated with the SSCA	13
3.4 Cyclic Feature Estimation with SSCA	17
4.0 RESULTS OF THE SSCA ENCODED IN C	19
4.1 Signal Descriptions	21
4.2 Theoretical Expected Results	22
4.3 Experimental Results	25
4.4 SSCA Benchmarks on a SUN IPX	38
5.0 SUMMARY AND CONCLUDING REMARKS	43
A.0 CYCLIC FEATURE DETECTION RESULTS	A-1
REFERENCES	REF-1

LIST OF FIGURES

		Page
Figure 1:	SSCA Implementation	10
Figure 2:	Mapping Visualization.	14
Figure 3:	SSCA Mapping Algorithm.	15
Figure 4:	Output Data File Format.	16
Figure 5:	CS of a BPSK Signal: Varying the Observation Time.	27
Figure 6:	CFF of a BPSK Signal: Varying the Observation Time.	28
Figure 7:	CS of a BPSK Signal: Varying the Frequency Resolution.	30
Figure 8:	CFF of a BPSK Signal: Varying the Frequency Resolution.	31
Figure 9:	CS of Noise: Varying the Observation Time.	32
Figure 10:	CFF of Noise: Varying the Observation Time.	33
Figure 11:	CS of Noise: Varying the Frequency Resolution.	34
Figure 12:	CFF of Noise: Varying the Frequency Resolution.	35
Figure 13:	CS of Various BPSK Signals Using N=32768, Np=64.	36
Figure 14:	CFF of Various BPSK Signals Using N=32768, Np=64.	37
Figure 15:	CS of Various BPSK Signals in Noise N0 Using N=32768, Np=64.	39
Figure 16:	CFF of Various BPSK Signals in Noise N0 Using N=32768, Np=64.	40
Figure 17:	CS of Various BPSK Signals in Noise N5 Using N=32768, Np=64.	41
Figure 18:	CFF of Various BPSK Signals in Noise N5 Using N=32768, Np=64.	42

LIST OF TABLES

		Page
Table 1:	SSCA Computational Requirements.	11
Table 2:	Options for the **ssca** Program.	20
Table 3:	Signals Parameters (for $f_s = 100$kHz).	21
Table 4:	Normalized Signals Parameters ($f_s = 1$Hz).	22
Table 5:	Theoretical Signals Cyclic Features Distribution.	26
Table 6:	Results of SSCA Benchmarks on a SUN IPX.	38
Table 7:	A (N=32768, Np=64), 21 Features Detected.	A-1
Table 8:	B (N=32768, Np=64), 15 Features Detected.	A-2
Table 9:	C (N=32768, Np=64), 9 Features Detected.	A-2
Table 10:	A+B+C (N=32768, Np=64), 35 Features Detected.	A-3
Table 11:	A+N0 (N=32768, Np=64), 15 Features Detected.	A-4
Table 12:	B+N0 (N=32768, Np=64), 14 Features Detected.	A-4
Table 13:	C+N0 (N=32768, Np=64), 9 Features Detected.	A-5
Table 14:	A+B+C+N0 (N=32768, Np=64), 31 Features Detected.	A-6
Table 15:	A+N5 (N=32768, Np=64), 15 Features Detected.	A-7
Table 16:	B+N5 (N=32768, Np=64), 9 Features Detected.	A-7
Table 17:	C+N5 (N=32768, Np=64), 9 Features Detected.	A-8
Table 18:	A+B+C+N5 (N=32768, Np=64), 27 Features Detected.	A-8

1.0 INTRODUCTION

Cyclic spectral analysis (CSA) as a general tool for signal analysis has been shown to be much superior to more conventional spectral analysis [1]. However, it is recognized that the computation of the entire cyclic spectrum (CS) is considerably more complex and time-consuming than the computation of the conventional power spectral density (PSD). The estimation of correlation between spectral components of signals as compared to only computing the spectral components themselves makes the CSA a computationally complex mechanism mainly because of the potentially large number of correlation computations involved. With the growing importance of CSA for many applications (cf.[2]), a search to derive efficient algorithms for computing the cyclic spectrum has been taking place over the last decade or so. These CS estimation algorithms divide mainly into two subgroups: the frequency-smoothing (FS) algorithms and the time-smoothing (TS) algorithms. More lately, algorithms merging the two methods have been used and are referred to as hybrid-smoothing algorithms [3]. These will not be discussed in this report.

Focusing on the problem of computing the entire CS, TS algorithms result in more computationally efficient algorithms than those involving FS.[1] Based on an analysis of the performance of the currently existing TS algorithms (in [4] and [3]), one particular TS algorithm called the Strip Spectral Correlation Algorithm (SSCA) has been chosen for implementation.

This report looks at the implementation of the SSCA for the computation of the entire CS. But first, some background on CS estimation for discrete-time signals is required.

2.0 BACKGROUND

In this section, the theory of spectral correlation necessary for CSA of discrete-time signals is reviewed. Fundamentally, there are two possible approaches for developing the theory of CSA: the probabilistic approach (cf.[5]) and the deterministic approach (cf.[6]).[2] Here, the deterministic framework is chosen because of its greater tractability

[1] Note that if the CS is required for only few values of known cycle frequency, FS algorithms can be computationally superior.

[2] In the deterministic framework, time averages are used as opposed to ensemble averages for the probabilistic framework.

and its natural link to practical problems [2] (e.g., signal processing of discrete-time communication signals for various applications).

The cyclic autocorrelation function of a discrete-time sequence $x(n)$ is defined as

$$R_x^\alpha(k) = \lim_{N\to\infty} \frac{1}{2N+1} \sum_{n=-N}^{n=N} \left[x(n+k)e^{-j\pi\alpha(n+k)}\right] \left[x(n)e^{j\pi\alpha n}\right]^* . \tag{1}$$

The sequence $x(n)$ is said to be wide sense cyclostationary if and only if $R_x^\alpha(k) \neq 0$ for some α. The CS $S_x^\alpha(f)$ is simply the Fourier Series Transform (FST) of $R_x^\alpha(k)$, i.e.,

$$S_x^\alpha(f) = \sum_{k=-\infty}^{\infty} R_x^\alpha(k)e^{-j2\pi fk} . \tag{2}$$

Defining α as the cycle frequency and f as the spectral frequency, $S_x^\alpha(f)$ can give rise to a three-dimensional plot with the three axes being: either $|S_x^\alpha(f)|$ or $\angle S_x^\alpha(f)$, f, and α. In general, $S_x^\alpha(f)$ is complex-valued.

2.1 Basic Frequency-smoothing Approach

The FS approach for computing $S_x^\alpha(f)$ is based on the double limit

$$S_x^\alpha(f) = \lim_{\Delta f\to 0} \lim_{\Delta t\to\infty} S_{x_{\Delta t}}^\alpha(n,f)_{\Delta f} , \tag{3}$$

where

$$S_{x_{\Delta t}}^\alpha(n,f)_{\Delta f} = \frac{1}{\Delta f} \int_{f-\frac{\Delta f}{2}}^{f+\frac{\Delta f}{2}} X_{\Delta t}(n,F+\alpha/2)X_{\Delta t}^*(n,F-\alpha/2)dF \tag{4}$$

is the frequency-smoothed cyclic periodogram and

$$X_{\Delta t}(n,f) = \frac{1}{\Delta t} \sum_{m=n-\frac{\Delta t}{2}}^{n+\frac{\Delta t}{2}} x(m)e^{-j2\pi fmT_s} \tag{5}$$

is referred to as the complex demodulate of $x(n)$, a discrete-time signal sampled at $f_s = 1/T_s$ Hz.

$S_{x_{\Delta t}}^\alpha(n,f)_{\Delta f}$ is the result of correlating spectral components of $x(n)$ over Δf Hz (i.e., averaging in frequency). The quantities Δf and Δt are respectively called the frequency and time resolution of the estimate. Note that $S_{x_{\Delta t}}^\alpha(n,f)_{\Delta f}$ is used for estimating

$S_x^\alpha(f)$ and a reliable estimate would have a large resolution product $\Delta t \Delta f$.

2.2 Basic Time-smoothing Approach

Using the TS approach, $S_x^\alpha(f)$ is also expressed as a double limit

$$S_x^\alpha(f) = \lim_{T\to\infty} \lim_{\Delta t\to\infty} S_{x_T}^\alpha(n,f)_{\Delta t} \tag{6}$$

where

$$S_{x_T}^\alpha(n,f)_{\Delta t} = \frac{1}{\Delta t} \sum_{m=n-\frac{\Delta t}{2}}^{n+\frac{\Delta t}{2}} X_T(m, f+\alpha/2) X_T^*(m, f-\alpha/2) \tag{7}$$

is the time-smoothed cyclic periodogram and

$$X_T(n,f) = \frac{1}{T} \sum_{m=n-\frac{T}{2}}^{n+\frac{T}{2}} x(m) e^{-j2\pi f m T_s} \tag{8}$$

is another form of the complex demodulate of $x(n)$ for a smaller time duration since $T \ll \Delta t$.

The TS cyclic periodogram $S_{x_T}^\alpha(n,f)_{\Delta t}$ is used to estimate $S_x^\alpha(f)$. As can be seen from (7), $S_{x_T}^\alpha(n,f)_{\Delta t}$ is, in fact, the discrete time-average of spectral correlation components of $x(n)$ over a time Δt. In this case, the frequency resolution is $\Delta f = 1/T$.

2.3 Comments on Both Approaches

Some comments with respect to both approaches have to be made.

1. The order of the double limit used to compute $S_x^\alpha(f)$ is <u>not</u> interchangeable.
2. It has been shown in [6] that FS and TS approaches are equivalent if and only if $\Delta t \Delta f \gg 1$, i.e., $S_{x_{\Delta t}}^\alpha(n,f)_{\Delta f} \approx S_{x_T}^\alpha(n,f)_{\Delta t}$ for $\Delta t \Delta f \gg 1$.
3. The condition $\Delta t \Delta f \gg 1$ is essential in order to obtain reliable estimates.
4. The particular choices of $\Delta t \Delta f$ and Δf depend on the signals under investigation (signals environment) and the degree of reliability which is needed.

Generally speaking, the goal is to find an efficient algorithm for high $\Delta t \Delta f$. In [4], it is shown that the SSCA (a TS algorithm) is one of the best derived so far for $\Delta t \Delta f > 128$, $\Delta f > 1/32$, and with a small $\Delta \alpha$ (the cycle frequency resolution).

3.0 THE STRIP SPECTRAL CORRELATION ALGORITHM

This section describes and analyses the SSCA.

3.1 From the Basic Time-smoothing Approach to the SSCA

Using a data tapering window $a(r)$ of length $T = N_p T_s$ seconds, the complex demodulate of $x(n)$ can be re-expressed as being

$$X_T(n,f) = \sum_{r=\frac{1-N_p}{2}}^{\frac{N_p}{2}} a(r)x(n-r)e^{-j2\pi f(n-r)T_s} \tag{9}$$

$$= \left[\sum_{r=\frac{-N_p}{2}}^{\frac{N_p}{2}-1} a(r)x(n+r)e^{-j2\pi f r T_s} \right] e^{-j2\pi f n T_s} \tag{10}$$

where T_s is the sampling period. The term in brackets represents the centered Fast Fourier Transform (FFT) of $x(n)$ using a window $a(r)$. Note that $\Delta f = \Delta a = f_s/N_p$ (where $\Delta a = \frac{1}{T}$ is the bandwidth of the input filters). Correlating the complex demodulates for a time $\Delta t = NT_s$ seconds, the TS cyclic periodogram is then given by

$$S_{x_T}^{\alpha}(n,f)_{\Delta t} = \sum_{m=-\frac{N}{2}}^{\frac{N}{2}-1} X_T\left(n+m, f+\frac{\alpha}{2}\right) X_T^*\left(n+m, f-\frac{\alpha}{2}\right) g(m) \tag{11}$$

where $g(m)$ is another data tapering window of length Δt. As mentioned earlier, for $S_{x_T}^{\alpha}(n,f)_{\Delta t}$ to be a reliable estimate of $S_x^{\alpha}(f)$, $\Delta t \Delta f \gg 1$ (i.e., $\Delta t \gg T$) is required. In the limit (i.e., $\Delta t \to \infty$ followed by $\Delta f \to 0$), if $a(n)$ and $g(n)$ are normalized such that

$$\sum_n a^2(n) = \sum_n g(n) = 1\,, \tag{12}$$

then $S_{x_T}^{\alpha}(n,f)_{\Delta t} = S_x^{\alpha}(f)$ [3].

In order to extend (11) to transform the averaging operation into an FFT , the

product sequence must be frequency shifted by an amount γ (i.e., from α to $\alpha+\gamma$). The result is then

$$S_{x_T}^{\alpha+\gamma}(n,f)_{\Delta t} = \sum_{m=-\frac{N}{2}}^{\frac{N}{2}-1} X_T\left(n+m, f+\frac{\alpha}{2}\right) X_T^*\left(n+m, f-\frac{\alpha}{2}\right) g(m) e^{-j2\pi\gamma m T_s}. \quad (13)$$

Using (13), one can find that $\Delta f = \Delta a - |\gamma|$ with $(|\gamma| \leq \Delta a)$, a non-uniform frequency resolution since several values of γ are usually required. If $\gamma = q\Delta\alpha$, then (13) becomes

$$S_{x_T}^{\alpha_i+q\Delta\alpha}(n,f_j)_{\Delta t} = \sum_{m=-\frac{N}{2}}^{\frac{N}{2}-1} X_T(n+m,f_k)\, X_T^*(n+m,f_l)\, g(m) e^{\frac{-j2\pi mq}{N}} \quad (14)$$

which is an N-point centered FFT. Note that $f_k = k(f_s/N_p)$, $k = -N_p/2, ..., (N_p/2)-1$, represents several frequencies for a complete coverage of the bifrequency plane (f,α). To relate f_j and α_i to f_k and f_l, the following relations are needed:

$$f_j = \frac{f_k+f_l}{2} = \frac{k+l}{2}\left(\frac{f_s}{N_p}\right) \quad (15)$$

and

$$\alpha_i = f_k - f_l = (k-l)\left(\frac{f_s}{N_p}\right). \quad (16)$$

For the Strip Spectral Correlation Algorithm (SSCA) [3][4][7][8], one has to set $\alpha_i = f_k$, $f_j = (f_k - q\Delta\alpha)/2$ and replace $X_T^*(n,f_l)$ by the unfiltered signal $x^*(n)$ in (14)[3] such that

$$S_{x_T}^{f_k+q\Delta\alpha}\left(n, \frac{f_k-q\Delta\alpha}{2}\right)_{\Delta t} = \sum_{m=-\frac{N}{2}}^{\frac{N}{2}-1} X_T(n+m,f_k)\, x^*(n+m)\, g(m) e^{\frac{-j2\pi qm}{N}}. \quad (17)$$

This allows Δf as well as $\Delta t\Delta f$ to be uniform, a highly desirable feature for the estimator. The points estimates produced by (17) will lie along the frequency-skewed family of lines $\alpha = 2f_k - 2f$ to result in a strip for each f_k. The following applies to the SSCA

[3]Note that this is done at the expense of minor degradation in output signal-to-noise ratio (cf.[7]). The estimate obtained in (17) is equivalent to (14) only if $\Delta f\Delta t \gg 1$, condition which is essential to have a reliable estimate anyway.

implementation:

$$\Delta f = 1/N_p,\ \Delta\alpha = 1/\Delta t = 1/N,\ \Delta f \Delta t = N/N_p,\ a(0) = \sum_n g(n) = 1, \tag{18}$$

and

$$\alpha = f_k + q\Delta\alpha,\ \ k = -\frac{N_p}{2}, ..., \frac{N_p}{2} - 1 \tag{19}$$

$$f = \frac{f_k - q\Delta\alpha}{2},\ \ q = -\frac{N}{2}, ..., \frac{N}{2} - 1\,. \tag{20}$$

Note that if the cross-cyclic spectrum (say between $x(n)$ and $y(n)$) is required instead of the auto-CS, then $x^*(n+m)$ in (17) simply becomes $y^*(n+m)$. In addition, if the conjuguate auto-CS and conjuguate cross-CS are desired, simply replace $x^*(n+m)$ and $y^*(n+m)$ by $x(n+m)$ and $y(n+m)$ in (17) respectively. It has been pointed out in [9] that since one of the channels is unfiltered, the complex demodulates have to come in at full rate, i.e. without decimation. It is, however, proposed in that particular paper to decimate the complex demodulates in order to reduce the number of input channelizers by incorporating a hold operation at the end of every channelizer. This method has been tried here by the author and it was found that the hold operation was introducing false cyclic features which, on the other hand, could possibly be predicted. The technique will not be discussed further in this paper but merits some considerations as it saves computation time and storage space.

3.2 SSCA Description

Based on (10) and (17) and assuming a single processor, the algorithm can be formulated in the following steps.

Step 1 Data collection:

- Collect a block of data of $N + N_p$ samples, i.e., $x(n)$, $n = 1, 2, \ldots, N + N_p$.

Step 2 Compute N N_p-point FFTs of sub-blocks of $x(n)$:

- Define $a(r)$ for $r = 1, 2, \ldots, N_p$ to be an N_p-point data-tapering window (e.g. rectangular, Hamming, Hanning, Kaiser ...).

- For $n = 1, 2, \ldots, N$, $r = 1, 2, \ldots, N_p$, and $k = -\frac{N_p}{2}, \ldots, \frac{N_p}{2} - 1$, compute

$$x_T(n,k) = \text{FFTS}_{N_p}\{a(r)x(n+r-1)\} \tag{21}$$

where FFTS_{N_p} is the N_p-point centered FFT operation (i.e., with the zero frequency in the $k = 0$ bin).

Step 3 Compute the weighted product from (17):

- Define $g(n)$ for $n = 1, 2, \ldots, N$ to be a N-point data-tapering window (e.g. as above).
- For $n = 1, 2, \ldots, N$ and $k = -\frac{N_p}{2}, \ldots, \frac{N_p}{2} - 1$, compute

$$X_g(n,k) = \underbrace{\overbrace{x_T(n,k)e^{-j\frac{2\pi(n-1)k}{N_p}}}^{\text{corrected FFTs as in (10)}} x^*\left(n + \frac{N_p}{2}\right)}_{\text{product}} \underbrace{g(n)}_{\text{weights}}. \tag{22}$$

Step 4 Compute the spectral correlation function:

- For $q = -\frac{N}{2}, \ldots, \frac{N}{2} - 1$, $k = -\frac{N_p}{2}, \ldots, \frac{N_p}{2} - 1$, and $n = 1, 2, \ldots, N$, compute

$$S_x(q,k) = \text{FFTS}_N\{X_g(n,k)\} \tag{23}$$

where FFTS_N is the N-point centered FFT operation (i.e., with the zero frequency in the $q = 0$ bin).

Step 5 Map $S_x(q,k)$ onto $S_x^\alpha(f)$:

- The mapping[4] is performed using the equations

$$\begin{cases} f = \frac{k}{2N_p} - \frac{q}{2N} \\ \alpha = \frac{k}{N_p} + \frac{q}{N} \end{cases} \tag{24}$$

where f and α are normalized with respect to $f_s = 1$, i.e.,

$$-0.5 \le f \le 0.5 \text{ and } -1 \le \alpha \le 1.^5 \tag{25}$$

[4]This mapping is absolutely required for plotting and interpreting the cyclic spectrum.

[5]Note that, really, $f_{min} \le f \le f_{max}$ where $f_{min} = -0.5 + \frac{1}{2N}$ and $f_{max} = 0.5 - \frac{1}{2N_p}$ while $\alpha_{min} \le \alpha \le \alpha_{max}$ where $\alpha_{min} = -1$ and $\alpha_{max} = 1 - \frac{1}{2N_p} - \frac{1}{2N}$.

This algorithm (as described from **Step 1–5**) can also be expressed in terms of matrix operations (or array processing). One possible formulation is presented below.

Step 1 Given the input data vector $\mathbf{x} = \left[\begin{array}{cccc} x(1) & x(2) & \cdots & x(N+N_p) \end{array} \right]$, create the NxN_p input data matrix $\mathbf{X}$ where

$$\mathbf{X} = \left[\begin{array}{cccc} x(1) & x(2) & \cdots & x(N_p) \\ x(2) & x(3) & \cdots & x(N_p+1) \\ \vdots & \vdots & \ddots & \vdots \\ x(N) & x(N+1) & \cdots & x(N+N_p) \end{array} \right]. \tag{26}$$

Step 2 Compute the N_p-point window row-vector $\mathbf{a} = \left[\begin{array}{cccc} a(1) & a(2) & \cdots & a(N_p) \end{array} \right]$ and create $\mathbf{A}$ (an NxN_p matrix) formed by N rows of $\mathbf{a}$. Knowing $\mathbf{A}$, compute $\mathbf{XA} = \mathbf{X} \odot \mathbf{A}$ where $\odot$ denotes the Hadamard product (i.e., element by element matrix multiplication). Then, compute

$$\mathbf{XA_T} = \text{MFFTS}_{N_p}\{\mathbf{XA}\} = \left[\begin{array}{c} \text{FFTS}_{N_p}\{\mathbf{xa}_1\} \\ \text{FFTS}_{N_p}\{\mathbf{xa}_2\} \\ \vdots \\ \text{FFTS}_{N_p}\{\mathbf{xa}_N\} \end{array} \right] \tag{27}$$

where

$$\mathbf{XA} = \mathbf{X} \odot \mathbf{A} = \left[\begin{array}{c} \mathbf{xa}_1 \\ \mathbf{xa}_2 \\ \vdots \\ \mathbf{xa}_N \end{array} \right] \tag{28}$$

and FFTS_{N_p} is as defined before.

Step 3 Compute the N-point window column-vector $\mathbf{g} = \left[\begin{array}{cccc} g(1) & g(2) & \cdots & g(N) \end{array} \right]^T$ and create $\mathbf{G}$ (an NxN_p matrix) formed by N_p columns of $\mathbf{g}$. Also, create the exponential matrix $\mathbf{E}$ as follows:

$$\mathbf{E} = \left[\begin{array}{cccc} e_{-\frac{N_p}{2},1} & e_{-\frac{N_p}{2}+1,1} & \cdots & e_{\frac{N_p}{2}-1,1} \\ e_{-\frac{N_p}{2},2} & e_{-\frac{N_p}{2}+1,2} & \cdots & e_{\frac{N_p}{2}-1,2} \\ \vdots & \vdots & \ddots & \vdots \\ e_{-\frac{N_p}{2},N} & e_{-\frac{N_p}{2}+1,N} & \cdots & e_{\frac{N_p}{2}-1,N} \end{array} \right], \tag{29}$$

where $e_{k,n} = e^{-j\frac{2\pi(n-1)k}{N_p}}$ for $k = -\frac{N_p}{2}, \ldots, \frac{N_p}{2} - 1$ and $n = 1, \cdots, N$. Then, create $\mathbf{X}^*$ which is defined as:

$$\mathbf{X}^* = \begin{bmatrix} x^*(\frac{N_p}{2}+1) & x^*(\frac{N_p}{2}+1) & \cdots & x^*(\frac{N_p}{2}+1) \\ x^*(\frac{N_p}{2}+2) & x^*(\frac{N_p}{2}+2) & \cdots & x^*(\frac{N_p}{2}+2) \\ \vdots & \vdots & \ddots & \vdots \\ x^*(\frac{N_p}{2}+N) & x^*(\frac{N_p}{2}+N) & \cdots & x^*(\frac{N_p}{2}+N) \end{bmatrix}, \tag{30}$$

where $x^*(n)$ is the complex conjugate of $x(n)$. Finally, compute

$$\mathbf{X_g} = \mathbf{X}\mathbf{A_T} \odot \mathbf{E} \odot \mathbf{X}^*, \tag{31}$$

also an NxN_p matrix.

Step 4 The cyclic spectrum in matrix form (but without mapping) is found to be

$$\mathbf{Sx} = \text{MFFTS}_N \{\mathbf{X_g}\}, \tag{32}$$

an NxN_p matrix where each element is denoted $s_{x_{k,q}}$ for $-\frac{N_p}{2} \leq k \leq \frac{N_p}{2} - 1$ and $-\frac{N}{2} \leq q \leq \frac{N}{2} - 1$.

Step 5 The last step is to map the elements of the matrix **Sx** onto $S_x^\alpha(f)$, i.e., $s_{x_{k,q}} \Rightarrow S_x^\alpha(f)$ where α and f are related to k and q as in (24).

As can be seen, this is a highly parallel algorithm suitable for implementation using parallel architectures. However, the mapping may not necessarily be a trivial task (see next section).

Although this paper does not intend to go into the details of a hardware architecture using VLSI technology, a block diagram of the implementation of the SSCA is presented in Figure 1. This provides a succinct and complete visual form of the SSCA.

3.3 SSCA Analysis

The analysis of the SSCA can be based on two different aspects: the computational requirements and the accuracy of the estimates. The problem of mapping associated with the SSCA is treated separately.

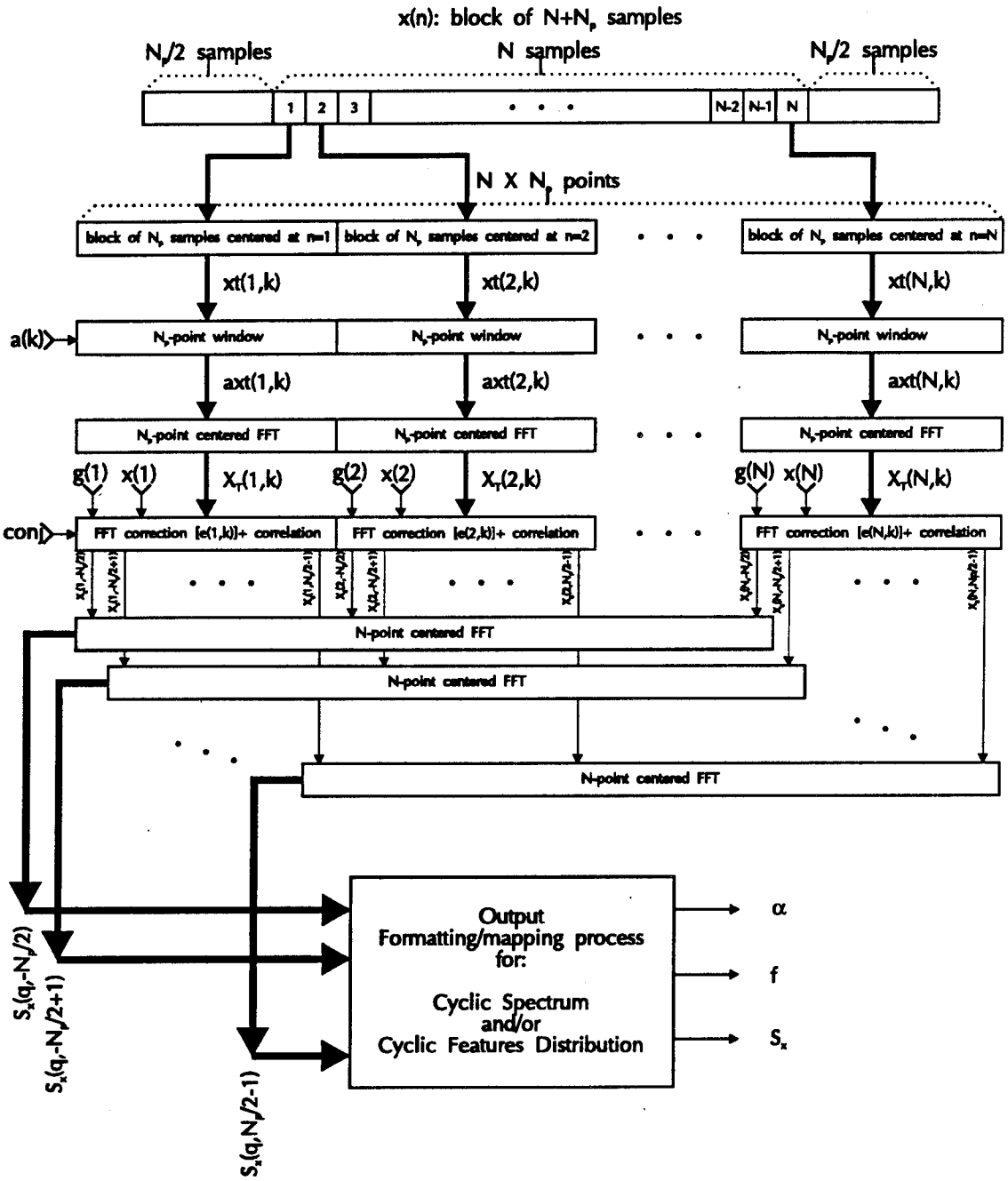

Figure 1: SSCA Implementation

Table 1: SSCA Computational Requirements.

Operation	# of Cmplx Mltply	# of Cmplx Addtn	# of Real Mltply	# of Real Addtn
Window $a(n)$	N_p	–	$2N_p$	–
N_p-point FFT	$\frac{N_p}{2}\log_2 N_p$	$N_p \log_2 N_p$	$2N_p \log_2 N_p$	$3N_p \log_2 N_p$
Down-convert+product	$2N_p$	–	$8N_p$	$4N_p$
Window $g(n)$	N	–	$2N$	–
N-point FFT	$\frac{N}{2}\log_2 N$	$N \log_2 N$	$2N \log_2 N$	$3N \log_2 N$

3.3.1 Computational Requirements

Analyzing the SSCA in terms of computational requirements boils down to analyzing the number of various arithmetic operations required for each steps of the algorithm. Note however that the analysis is made with respect to sequential computations requirements.

Assuming $a(r)$ and $g(n)$ are already defined before the beginning of the algorithm, the number of arithmetic operations required for each step (ignoring the mapping operation) would be as given in Table 1.[6] Note that the arithmetic operations under investigation are complex multiplications and complex additions which are transposed into real multiplications and real additions in the two last columns.

Denoting the total number of real multiplies and additions for the single-processor as C_{rm}^s and C_{ra}^s respectively, then the computational requirements are found to be

$$C_{rm}^s = F(2 + 2\log_2 F) \tag{33}$$

and

$$C_{ra}^s = F(4 + 3\log_2 F)\,, \tag{34}$$

where $F = N \cdot N_p$.[7] Now, for a multi-processor architecture (although not necessarily

[6] A radix-2 FFT algorithm is used.

[7] For the single-processor, the first three operations in Table 1 are performed N times and the last two, N_p times.

optimized), the computational requirements are

$$C_{rm}^{m} = N_p\,(10 + 2\log_2 N_p) + N\,(2 + 2\log_2 N) \tag{35}$$

and

$$C_{ra}^{m} = N_p\,(4 + 3\log_2 N_p) + N\,(3\log_2 N) \tag{36}$$

where C_{rm}^{m} and C_{ra}^{m} are the multi-processor equivalent of C_{rm}^{s} and C_{ra}^{s}. Note that if $x(n)$ is assumed to be a real signal, these figures will go down. Clearly, the possibility of using a parallel architecture with the SSCA reduces considerably the computational requirements.

3.3.2 Accuracy of the Estimates

The accuracy of the SSCA for estimating the cyclic spectrum is related to the parameters N, N_p, and the type of data tapering window chosen, i.e., $a(n)$ and $g(n)$. The frequency resolution, Δf, the cycle frequency resolution, $\Delta\alpha$, and the resolution product, $\Delta f \Delta t$ are all specified in terms of N and N_p as stated in (18). However, the choice of $a(n)$ and $g(n)$ will impact on the accuracy of the point estimates. Essentially, the bandwidth of $a(n)$ is assumed to be $\Delta a = 1/N_p$ (assuming $f_s = 1$) and the bandwidth of $g(n)$, $\Delta g = 1/N$. The kernel transform associated with the SSCA is found from (17) and is given by [3][4][8]

$$M(\alpha, f) = G(\alpha - \alpha_0) A\left(f - f_0 + \frac{\alpha - \alpha_0}{2}\right), \tag{37}$$

where $G(\cdot)$ and $A(\cdot)$ are the Fourier Transforms of $g(n)$ and $a(n)$ respectively. Also recall that

$$\alpha_0 = \frac{k}{N_p} + \frac{q}{N} \tag{38}$$

$$f_0 = \frac{k}{2N_p} - \frac{q}{2N} \tag{39}$$

where $k = -N_p/2, \ldots, N_p/2 - 1$ and $q = -N/2, \ldots, N/2 - 1$ (again assuming $f_s = 1$). As a result, $A\left(f - f_0 + \frac{\alpha - \alpha_0}{2}\right)$ is a strip approximately Δa wide along the line $\alpha = 2f_k - 2f$ (where $f_k = k/N_p$). This implies that all point estimates have a constant frequency resolution of $\Delta f = \Delta a$. In addition, they also possess a constant cycle frequency resolution which is determined by $G(\alpha)$, i.e., $\Delta\alpha = 1/N$.

In practice, $a(n)$ or $g(n)$ will never produce perfect bandpass filters and some parameters such as bandwidth and attenuation are always associated with practical filters. A judicious choice for the best windows to use is easier to make by experimentation. The family of Kaiser windows allows (via the parameter β) various attenuations and therefore constitutes a good choice for experimentation. As a general conclusion coming out of these investigations, it is important that $a(n)$ has a large attenuation while $g(n)$ has a small bandwidth characteristic. Since both attenuation and bandwidth are intimately related, obtaining a larger attenuation is equivalent to trading-off the bandwidth (i.e., getting a larger bandwidth) and vice-versa. As a result, $a(n)$ will have a large attenuation but also a large bandwidth and $g(n)$ a small bandwidth but also a small attenuation.

3.3.3 Mapping Associated with the SSCA

One important issue of the SSCA concerns the mapping operation as briefly explained in **Step 5**. This will now be discussed in more depth.

Before going into the details of the algorithm required for the mapping, the region of support for the cyclic spectrum in the bifrequency plane is first examined. This is done by visualizing the mapping of k and q onto f and α in Figure 2. In Figure 2(a), $N = 32$ and $N_p = 8$ are used and therefore $k = -4, \ldots, 3$ and $q = -16, \ldots, 15$. Each point in this bifrequency plane represents a point estimate and is located at the center of a rectangle having widths $\Delta a = 1/N_p$ on the f-axis and $\Delta\alpha = 1/N$ on the α-axis. Note that f is minimum at $q = 15$ $(= \frac{N}{2} - 1)$ and $k = -4$ $(= \frac{-N_p}{2})$, and is maximum at $q = -16$ $(= -\frac{N}{2})$ and $k = 3$ $(= \frac{N_p}{2} - 1)$, while α is minimum at $q = -16$ and $k = -4$, and is maximum at $q = 15$ and $k = 3$. As can be seen, each negative-slope diagonal corresponds to a strip for a particular value of k (the bottom diagonal being $k = -N_p/2$ and the top one $k = N_p/2 - 1$). Each strip contains all the q values starting from the top of any strip at $q = -N/2$ to $q = N/2 - 1$ at the bottom. Figure 2(b) shows the mapping for higher N and N_p, providing smaller Δa and $\Delta\alpha$ (i.e., higher frequency resolutions). Some useful observations are noted: (1) all the point estimates having the same value of α will form the continuous spectrum related to this particular cycle frequency (recall that the cyclic spectrum is discretely distributed along the cycle frequency); (2) geometrically, the region of support is found to be a diamond (with the range of α being twice that of f) in the bifrequency plane; and (3) this diamond is not perfect in the sense that the corners of the diamond clearly do not align. The coverage on the negative and positive frequency is not the same but, nevertheless, as N and N_p goes to infinity, it tends to cover almost the

same region on both sides.

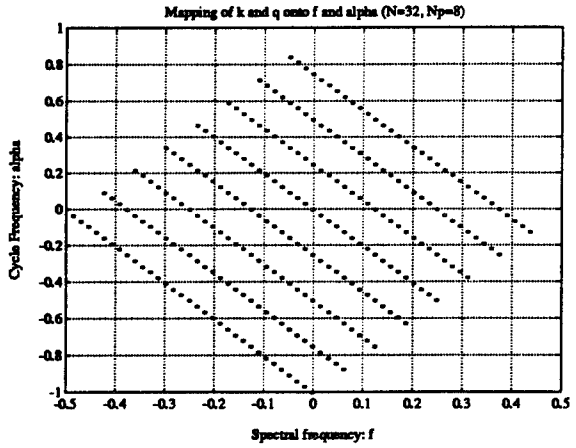

(a)

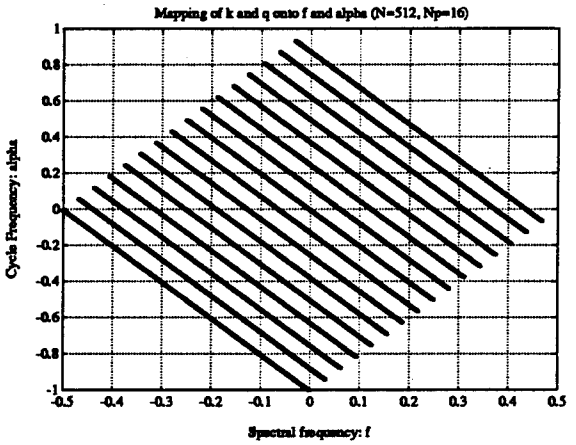

(b)

Figure 2: Mapping Visualization.

An algorithm for implementing the mapping operation is derived in Figure 3. To start with, the algorithm assumes that $S_x(q,k)$ (from **Step 4**) has been computed and is available. Then, a good strategy for storing that data for any further use (as for plotting or analysis) is to store the points estimates for each α. Therefore, the output data format is chosen to be as follows: a global header, followed by a slice header (for each α) and the points estimates values for this slice with this latter process repeated

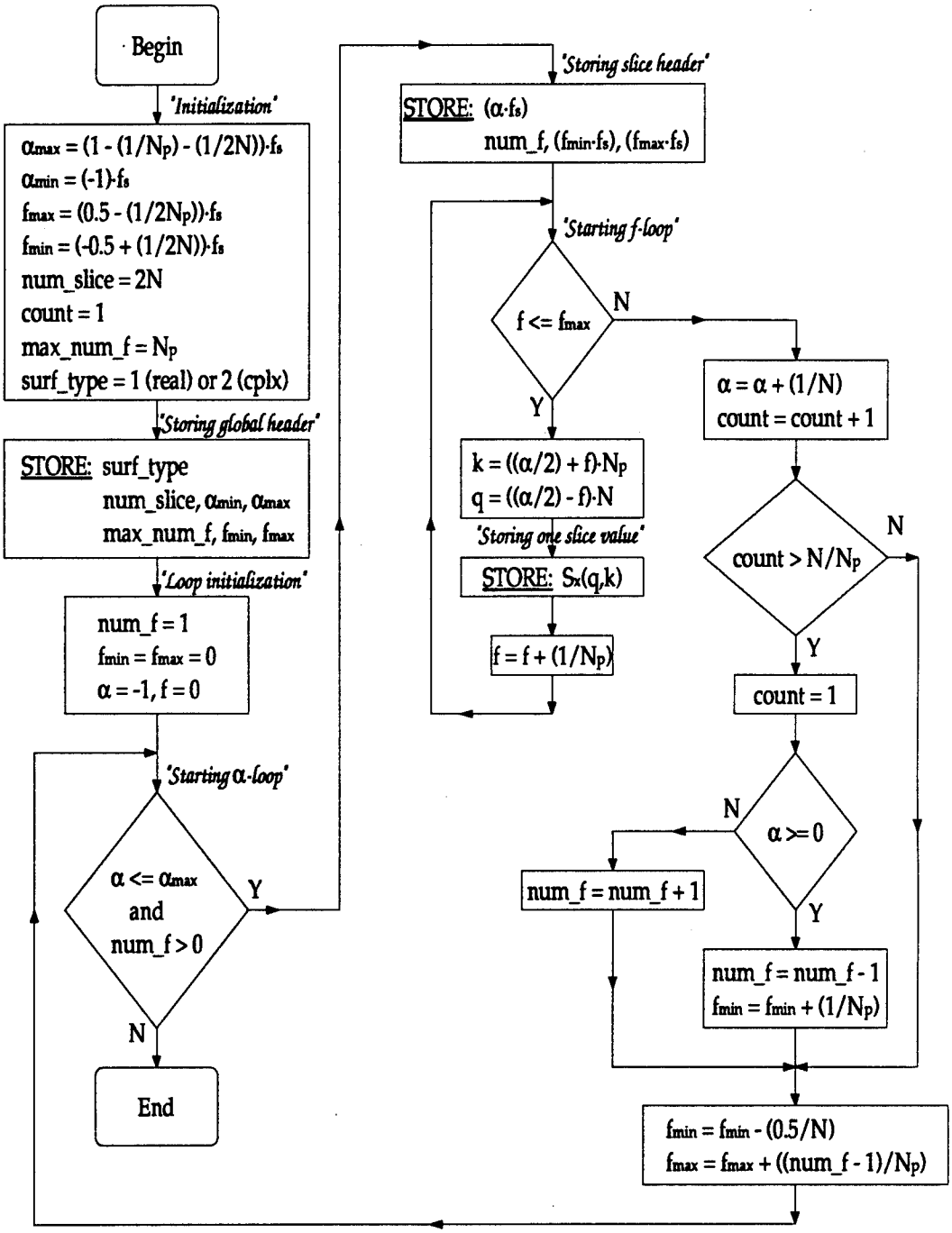

Figure 3: SSCA Mapping Algorithm.

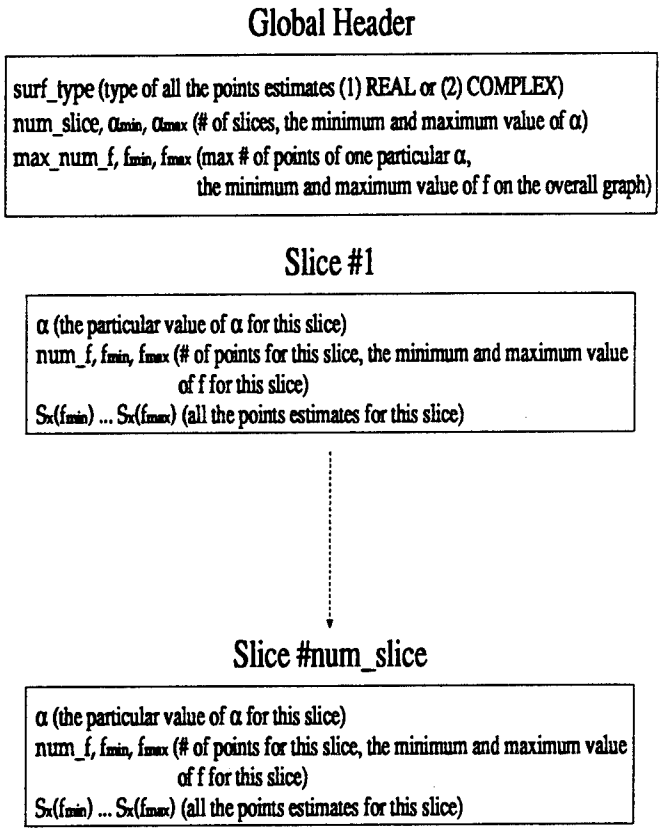

Figure 4: Output Data File Format.

for all slices (see Figure 4).[8] The algorithm maps the points estimates using this format and thus enters a loop for each value of α (the α-loop) and then an inner-loop (the f-loop) for each value of f possible according to this particular α. It takes into account all useful geometrical information found from the region of support investigation above and represents an effective way of mapping the data. Note however that if visualization of the CS is not required, then a very simple skew storage mechanism would align all points estimates with respect to α only.[9]

3.4 Cyclic Feature Estimation with SSCA

The CS constitutes a nice tool for spectral analysis of second-order wide sense cyclostationary signals. However, it is often necessary to only identify the cyclic features. In fact, all signal processing methods exploiting cyclostationary properties of signals (eg cyclic direction finding methods) require at least reliable estimates of the signal of interest's cyclic features in order for them to be useful. One can derive the second-order cyclic features from the CS estimate such as the one produced with the SSCA.

With the SSCA, the number of point estimates in the CS is $N \times N_p$ but the cycle frequency resolution is equal to $\frac{1}{N} \times f_s$ Hz. The maximum number of points used for detecting cyclic features should therefore be no greater than N in the case of real signals and $2N - \frac{N}{N_p}$ for complex signals. Such functions are defined below.

The simplest function is the max-cut function, defined by the author to be

$$\mathrm{MAX}(\alpha) \triangleq \max_f \left[|S_x^\alpha(f)|^2 \right] . \tag{40}$$

It retains the maximum magnitude squared of each α-cut. The max-cut function can easily be modified into

$$\mathrm{LM}(\alpha) \triangleq 10 \log_{10} \left[\frac{\mathrm{MAX}(\alpha)}{\mathrm{MAX}(0)} \right] \tag{41}$$

which is hereinafter referred to as the normalized log max-cut (NLMC) function. It is easily seen that

$$\mathrm{LM}(0) = 0 \tag{42}$$

[8]This output data file format is used as an input by the plot_sxaf program to plot the cyclic spectrum. This software is sold by Statistical Signal Processing Inc. (SSPI).

[9]This could be the case for example when hardware implementation is required and that the cyclic spectrum is used to detect cyclic features.

and furthermore

$$\mathrm{LM}(\alpha) \leq 0 \tag{43}$$

since MAX(0) should be greater to or equal to MAX(α). Even though these functions could be successfully used in practice to detect cyclic features, the best theoretical function (or measure) is called the cycle-frequency decomposed measure of degree of cyclostationarity and is given by [10]

$$\mathrm{DCS}^{\alpha} \triangleq \frac{\int_{-\infty}^{\infty} |S_x^{\alpha}(f)|^2 \, df}{\int_{-\infty}^{\infty} |S_x^{0}(f)|^2 \, df} = \frac{\int_{-\infty}^{\infty} |R_x^{\alpha}(\tau)|^2 \, d\tau}{\int_{-\infty}^{\infty} |R_x^{0}(\tau)|^2 \, d\tau}. \tag{44}$$

An estimate of this measure found from the CS estimate given by the SSCA is defined here to be

$$D(\alpha) \triangleq w(\alpha) \cdot \frac{\sum_f |S_x^{\alpha}(f)|^2}{\sum_f |S_x^{0}(f)|^2} \tag{45}$$

where $w(\alpha)$ denotes a weighting function of α. This weighting function takes into consideration the reliability of the CS measurement at α. Using

$$w(\alpha) = \frac{\mathrm{numf}(\alpha)}{\mathrm{numf}(0)} \tag{46}$$

with numf(α) denoting the number of point estimates computed at α, the effect of the varying number of points along α introduces a false relationship between the cyclic feature strengths. Specifically, going from $\alpha = 0$ to $\alpha = \pm 1$, the cyclic features strength would decrease even if they should be equal in reality. A way of avoiding this is to make sure the signal does not have any frequency component higher than $fs/4$ or lower than $-fs/4$ and consider the CS cuts only from $\alpha = -f_s/2$ to $\alpha = f_s/2$, therefore making the number of points to be added for each cut constant. This is equivalent to interpolating the signal by two and considering only the SSCA points estimates lying within the rectangular region $f_s/2 \leq \alpha \leq f_s/2$, $-f_s/4 \leq f \leq f_s/4$. Consequently, $w(\alpha) = 1$. This method however will double the number of points to be considered in the SSCA and complicates the realization of the algorithm. The author has tried another way of estimating DCS^{α} with the SSCA points estimates. Since DCS^{α} is resulting from a ratio of infinite integrals, it could easily be seen as a ratio of the averaged power at each cut and the averaged power at $\alpha = 0$. To realize this, we simply have to set

$$w(\alpha) = \frac{\mathrm{numf}(0)}{\mathrm{numf}(\alpha)}. \tag{47}$$

Nevertheless, this estimate suffers from reliability problems as we approach $\alpha = \pm f_s$ since less points are taken into account in the averaging operation and that the feature will get amplified by noisy points. As a result, the estimate using

$$w(\alpha) = 1 \tag{48}$$

seems to be the compromise. From a cyclic feature detection point of view, this last estimation method will be adequate and reliable but if someone is looking for feature strength relationships, a method similar to the one described above and using interpolation may be required.

Again, this measure can be represented in dB by taking the logarithm, i.e.

$$\mathrm{LD}(\alpha) \triangleq 10 \log_{10} \mathrm{D}(\alpha) \tag{49}$$

or equivalently

$$\mathrm{LD}(\alpha) = 10 \log_{10} \left[\sum_f |S_x^\alpha(f)|^2 \right] - C \tag{50}$$

where C is given by

$$C = 10 \log_{10} \left[\sum_f \left| S_x^0(f) \right|^2 \right] . \tag{51}$$

This measure provides a more reliable function for studying the signals cyclic features distribution and should, as the NLMC function, always be smaller or equal to 0 ($\mathrm{LD}(\alpha) \leq 0$). As a result, $\mathrm{LD}(\alpha)$, hereinafter referred to as the Cyclic Feature Function (CFF), is preferred.

4.0 RESULTS OF THE SSCA ENCODED IN C

The algorithm explained in the last section has been encoded in the C language on a SUN IPX computer. The program is called **ssca** and its usage is given as follows:

ssca [options] filename1 [filename2]

The filename1 is the name of the source file containing the block of samples of the signal to be analyzed. The second optional file name, filename2, is required only when the cross-correlation cyclic spectrum is computed. The different options that can be used are listed in Table 2.

Table 2: Options for the **ssca** Program.

Options	Description
-a *value*	specifies the amount of attenuation (in dB) for the 1st Kaiser window (Np samples long) - [Default ⇒ 96.0 dB]
-b *value*	specifies the amount of attenuation (in dB) for the 2nd Kaiser window (N samples long) - [Default ⇒ 20.0 dB]
-C	computes the conjuguate cyclic spectrum
-c	computes the cross-correlation cyclic spectrum (filename2 must be specified in this case)
-f *char*	specifies the format of the data to be produced in the output files (if *char* = a, the output is ASCII and if *char* = b, it is binary) - [Default ⇒ b]
-help	displays information on how to obtain on line help
-M	in addition to the cyclic spectrum output, also outputs the maximum value of the cyclic spectrum for each cycle frequency in a separate output file (using extension .max)
-N *value*	specifies the number of data samples being analyzed (i.e., N samples) - [Default ⇒ 1024]
-P *value*	specifies the number of data samples used in the channelizer (i.e., Np samples) - [Default ⇒ 8]
-o *file*	specifies the output file name - [Default ⇒ surf_out]
-d	in addition to the cyclic spectrum output, also outputs the degree of cyclostationarity for each cycle frequency in a separate output file (using extension .int)
-z	in addition to the cyclic spectrum output, also outputs the value of the cyclic spectrum at the zero frequency (or closest to zero) for each cycle frequency in a separate output file (using extension .zero)
-s *value*	decimates the number of output spectrum cut to *value* cuts without affecting the resolution. - [Default ⇒ 1024]

Table 3: Signals Parameters (for $f_s = 100$kHz).

Signal	Keying Rate	Carrier Frequency	Pulse Type $q(t)$	Bandwidth	Power (dBW)
A	4800 bauds	23 kHz	rect BL	4*4800	0.0
B	10000 bauds	23.5 kHz	rect BL	3*10000	0.0
C	9000 bauds	29.5 kHz	rect BL	2*9000	0.0
N0	--	--	--	$f_s/2$	0.0
N5	--	--	--	$f_s/2$	5.0

Using the **ssca** program, this section will compare cyclic spectrum results with theoretical expectations. Note that the program used to display the 3-dimensional spectrum is called **plot_sxaf** and is sold by Statistical Signal Processing Inc along with another type of cyclic spectral estimation algorithm using direct frequency-smoothing.

4.1 Signal Descriptions

The type of signal used for the analysis is the popular Phase-Shift Keying (PSK) modulated signal. Specifically, binary PSK (BPSK) modulated signals are used with additive white Gaussian noise (AWGN). A BPSK signal can be mathematically described in terms of pulse-amplitude modulation (PAM) as

$$x(t) = a(t)\cos\left(2\pi f_c t + \phi_0\right) , \tag{52}$$

where the signal envelope $a(t)$ is given by

$$a(t) = \sum_{n=-\infty}^{\infty} a_n q(t - nT_K - t_0) . \tag{53}$$

Note that a_n is a binary sequence (± 1), $q(t)$ is a finite energy keying envelope, and $T_K = 1/f_K$ is the symbol period expressed in seconds/symbols.[10] Table 3 and Table 4 describe three BPSK and two noise signals under investigation, along with their specific parameters.

[10]Note that 1 baud corresponds to 1 symbol/sec.

Table 4: Normalized Signals Parameters ($f_s = 1$Hz).

Signal	Keying Rate	Carrier Frequency	Pulse Type $q(t)$	Bandwidth	Power (dBW)
A	0.048	0.23	rect BL	4*0.048	0.0
B	0.1	0.235	rect BL	3*0.09	0.0
C	0.09	0.295	rect BL	2*0.1	0.0
N0	--	--	--	$f_s/2$	0.0
N5	--	--	--	$f_s/2$	5.0

4.2 Theoretical Expected Results

The theoretical CS of a BPSK signal is well known [11] and is derived below. We have

$$
\begin{aligned}
R_x^\alpha(\tau) &= \left\langle x(t+\tau/2)x(t-\tau/2)e^{-j2\pi\alpha t}\right\rangle \\
&= \left\langle a(t+\tau/2)\cos\left[2\pi f_c(t+\tau/2)+\phi_0\right]a(t-\tau/2)\cos\left[2\pi f_c(t-\tau/2)+\phi_0\right]e^{-j2\pi\alpha t}\right\rangle \\
&= \left\langle a(t+\tau/2)a(t-\tau/2)\frac{1}{2}\left[\cos(2\pi f_c\tau)+\cos(4\pi f_c t+2\phi_0)\right]e^{-j2\pi\alpha t}\right\rangle \\
&= \left\langle \frac{1}{2}a(t+\tau/2)a(t-\tau/2)\cos(2\pi f_c\tau)e^{-j2\pi\alpha t}\right\rangle \\
&\quad + \left\langle \frac{1}{2}a(t+\tau/2)a(t-\tau/2)\cos(4\pi f_c t+2\phi_0)e^{-j2\pi\alpha t}\right\rangle \\
&= \frac{1}{2}R_a^\alpha(\tau)\cdot\cos(2\pi f_c\tau) \\
&\quad + \left\langle \frac{1}{2}a(t+\tau/2)a(t-\tau/2)\cdot\frac{e^{j(4\pi f_c t+2\phi_0)}+e^{-j(4\pi f_c t+2\phi_0)}}{2}\cdot e^{-j2\pi\alpha t}\right\rangle \\
&= \frac{1}{2}R_a^\alpha(\tau)\cdot\cos(2\pi f_c\tau) \\
&\quad + \frac{1}{4}\left\langle a(t+\tau/2)a(t-\tau/2)e^{-j2\pi(\alpha-2f_c)t}e^{j2\phi_0}+a(t+\tau/2)a(t-\tau/2)e^{-j2\pi(\alpha+2f_c)t}e^{-j2\phi_0}\right\rangle \\
&= \frac{1}{2}R_a^\alpha(\tau)\cdot\cos(2\pi f_c\tau)+\frac{1}{4}R_a^{\alpha-2f_c}(\tau)\cdot e^{j2\phi_0}+\frac{1}{4}R_a^{\alpha+2f_c}(\tau)\cdot e^{-j2\phi_0}
\end{aligned}
\tag{54}
$$

where $R_a^\alpha(\tau)$ is the cyclic autocorrelation of the PAM signal $a(t)$. Using the cyclic Wiener relation, one can find the CS of $x(t)$ by Fourier transforming $R_x^\alpha(\tau)$, i.e.,

$$
S_x^\alpha(f) = \mathcal{F}\{R_x^\alpha(\tau)\} \tag{55}
$$

$$= \frac{1}{4}\left[S_a^\alpha(f-f_c) + S_a^\alpha(f+f_c) + S_a^{\alpha-2f_c}(f)\cdot e^{j2\phi_0} + S_a^{\alpha+2f_c}(f)\cdot e^{-j2\phi_0}\right] .$$

For $a(t)$ as expressed in (53), its CS is found to be

$$S_a^\alpha(f) = \begin{cases} \frac{1}{T_k} Q(f+\alpha/2)Q^*(f-\alpha/2)\tilde{S}_a(f+\alpha/2)e^{-j2\pi\alpha t_0} & , \alpha = p/T_K \\ 0 & , \text{otherwise} \end{cases} \tag{56}$$

where p is an integer, $Q(f) = \mathcal{F}\{q(t)\}$, $\tilde{S}_a(f) = \sum_{k=-\infty}^{k=\infty} \tilde{R}_a(k)\exp(-j2\pi k f T_K)$ and $\tilde{R}_a(k) = < a_{k+n}a_n >$ (discrete-time average of the sequence over n).[11] Using these results, we can then express $S_x^\alpha(f)$ as

$$S_x^\alpha(f) = \begin{cases} \frac{1}{4T_K}\Big[Q(f-f_2)Q^*(f-f_1)\tilde{S}_a(f-f_2) & \\ +Q(f+f_1)Q^*(f+f_2)\tilde{S}_a(f+f_1)\Big]\cdot e^{-j2\pi\alpha t_0} & , \alpha = p/T_K \\ & \\ \frac{1}{4T_K}\Big[Q(f-f_2)Q^*(f+f_2)\tilde{S}_a(f-f_2)e^{j[4\pi f_c t_0 + 2\phi_0]} & \\ +Q(f+f_1)Q^*(f-f_1)\tilde{S}_a(f+f_1)e^{-j[4\pi f_c t_0+2\phi_0]}\Big]\cdot e^{-j2\pi\alpha t_0} & , \alpha = \pm 2f_c + p/T_K \end{cases} \tag{57}$$

where

$$\begin{aligned} f_1 &= f_c + \alpha/2 \\ f_2 &= f_c - \alpha/2 . \end{aligned}$$

This is the general expression for the CS of a BPSK modulated signal as expressed in (52) and (53).

The actual choice of $q(t)$ (i.e., a band-limited rectangular pulse) is given by

$$q(t) = \text{rect}_{T_K}(t) * h_{lp}(t) \tag{58}$$

or equivalently

$$Q(f) = \frac{\sin(\pi f T_K)}{\pi f}\cdot H_{lp}(f) \tag{59}$$

where $\text{rect}_{T_K}(t)$ is defined as being the rectangular pulse of time duration T_K and $h_{lp}(t)$ is

[11] Note that for $\{a_n\} = \pm 1$ and independently identically distributed (i.i.d.), $\tilde{S}_a(f) = 1$.

the impulse response of the filter band-limiting the signal having $H_{lp}(f)$ as its frequency response. Replacing $Q(f)$ in the expression for the CS gives

$$S_x^\alpha(f) = \begin{cases} \frac{e^{-j2\pi\alpha t_0}}{4T_K}\Big[\frac{\sin(\pi(f-f_2)T_K)\cdot\sin(\pi(f-f_1)T_K)}{\pi(f-f_2)\cdot\pi(f-f_1)} \\ \cdot H_{lp}(f-f_2)H_{lp}(f-f_1)\tilde{S}_a(f-f_2) \\ +\frac{\sin(\pi(f+f_1)T_K)\cdot\sin(\pi(f+f_2)T_K)}{\pi(f+f_1)\cdot\pi(f+f_2)} \\ \cdot H_{lp}(f+f_1)H_{lp}(f+f_2)\tilde{S}_a(f+f_1)\Big] & , \alpha = p/T_K \\ \\ \frac{e^{-j2\pi\alpha t_0}}{4T_K}\Big[\frac{\sin(\pi(f-f_2)T_K)\cdot\sin(\pi(f+f_2)T_K)}{\pi(f-f_2)\cdot\pi(f+f_2)} \\ \cdot H_{lp}(f-f_2)H_{lp}(f+f_2)\tilde{S}_a(f-f_2)\cdot e^{j(4\pi f_c t_0+2\phi_0)} \\ +\frac{\sin(\pi(f+f_1)T_K)\cdot\sin(\pi(f-f_1)T_K)}{\pi(f+f_1)\cdot\pi(f-f_1)} \\ \cdot H_{lp}(f+f_1)H_{lp}(f-f_1)\tilde{S}_a(f+f_1)\cdot e^{-j(4\pi f_c t_0+2\phi_0)}\Big] & , \alpha = \pm 2f_c + p/T_K \\ \\ 0 & , \text{otherwise} \end{cases} \tag{60}$$

and furthermore, choosing the sequence $\{a(n)\}$ of ± 1 to be independently identically

distributed (i.i.d.) causes $\tilde{S}_a(f) = 1$, and therefore $S_x^\alpha(f)$ reduces to

$$S_x^\alpha(f) = \begin{cases} \frac{e^{-j2\pi\alpha t_0}}{4T_K} \left[\frac{\sin(\pi(f-f_2)T_K)\cdot\sin(\pi(f-f_1)T_K)}{\pi(f-f_2)\cdot\pi(f-f_1)} \right. \\ \cdot H_{lp}(f-f_2)H_{lp}(f-f_1) \\ \left. + \frac{\sin(\pi(f+f_1)T_K)\cdot\sin(\pi(f+f_2)T_K)}{\pi(f+f_1)\cdot\pi(f+f_2)} \right. \\ \left. \cdot H_{lp}(f+f_1)H_{lp}(f+f_2) \right] & , \alpha = p/T_K \\ \\ \frac{e^{-j2\pi\alpha t_0}}{4T_K} \left[\frac{\sin(\pi(f-f_2)T_K)\cdot\sin(\pi(f+f_2)T_K)}{\pi(f-f_2)\cdot\pi(f+f_2)} \right. \\ \cdot H_{lp}(f-f_2)H_{lp}(f+f_2)\cdot e^{j(4\pi f_c t_0 + 2\phi_0)} \\ \left. + \frac{\sin(\pi(f+f_1)T_K)\cdot\sin(\pi(f-f_1)T_K)}{\pi(f+f_1)\cdot\pi(f-f_1)} \right. \\ \left. \cdot H_{lp}(f+f_1)H_{lp}(f-f_1)\cdot e^{-j(4\pi f_c t_0 + 2\phi_0)} \right] & , \alpha = \pm 2f_c + p/T_K \\ \\ 0 & , \text{otherwise} \end{cases} \tag{61}$$

This last expression shows that the BPSK will have spectral correlation components at $\alpha = p/T_K$ and $\alpha = \pm 2f_c + p/T_K$ (for any integer p). In addition, the CS should look like a sinc-squared function at $\alpha = 0$ ($f = \pm f_c$) and $\alpha = \pm 2f_c$ ($f = 0$), band-limited by the bandwidth of the filter. For $p \neq 0$, the CS more or less corresponds to spectral correlation due to the p^{th} lobe of the spectrum. Since the number of lobes is band-limited to the bandwidth of the filter, the number of spectral correlation terms will be reduced accordingly. The expected cyclic features for each signal as described in Table 4 are shown in Table 5.[12]

4.3 Experimental Results

In this section, the CSs of the various generated signals (A, B, C, N0, and N5) are computed using the **ssca** program. The effects of varying some parameters in the algorithm are investigated. All CS 3D-plots only show $|S_x^\alpha(f)|$ on a linear scale. The f-axis and α-axis appear on the left and right side of the graph respectively. Also note that,

[12]In the table, f denotes the center frequency at which a cyclic feature is present.

Table 5: Theoretical Signals Cyclic Features Distribution.

Cyclic Feature	A	B	C
$\alpha = 0$	$f = \pm 0.23$	$f = \pm 0.235$	$f = \pm 0.295$
$\alpha = \pm p/T_K$	$\alpha = \pm 0.048 \cdot p$ $f = \pm 0.23$	$\alpha = \pm 0.1 \cdot p$ $f = \pm 0.235$	$\alpha = \pm 0.09 \cdot p$ $f = \pm 0.295$
$\alpha = \pm 2f_c$	$\alpha = \pm 0.46$ $f = 0$	$\alpha = \pm 0.47$ $f = 0$	$\alpha = \pm 0.59$ $f = 0$
$\alpha = \pm 2f_c + p/T_K$	$\alpha = \pm 0.46 \pm 0.048 \cdot p$ $f = 0$	$\alpha = \pm 0.47 \pm 0.1 \cdot p$ $f = 0$	$\alpha = \pm 0.59 \pm 0.09 \cdot p$ $f = 0$

since the option **-s 512** has been used to reduce the large number of points generated by the algorithm, the number of output cuts has been decimated to 512 cuts for each reported result.

The effect of varying the observation time (N) on the CS of signal A is shown in Figure 5. First, increasing the observation time increases the strength of the spectral correlation terms, provided the signal is present for the entire observation time (which is the case here). Second, since N_p is kept fixed in this case, increasing N corresponds to increasing $\Delta t \Delta f$ ($= N/N_p$). Figure 5(a) clearly shows undesired spectral components (due to measurement unreliability). Starting from (c) ($\Delta t \Delta f = 16384/64 = 256$), the CS appears free of these unwanted components and therefore seems to be a reliable measurement (qualitatively).

Even though the CS 3D-plot is a useful for spectral analysis of cyclostationary signals, another plot derived from the CS and more suitable for cyclic features detection has been defined in an earlier section. This function, the CFF (=LD(α)), estimates the cycle frequency-decomposed measure of the DCS or equivalently represents the cyclic feature strengths in dB distributed over α. This function was produced with the **ssca** program by using the option *-d*. As shown in Figure 6, the CFF graphs (using the same parameters conditions as the previous figure) provide better pictures for studying the cyclic features along α.[13] The spectral shape however is lost. In this section, the CFF

[13]The CFF graphs show a dashed line arbitrarily set to -40 dB representing the minimum value for a

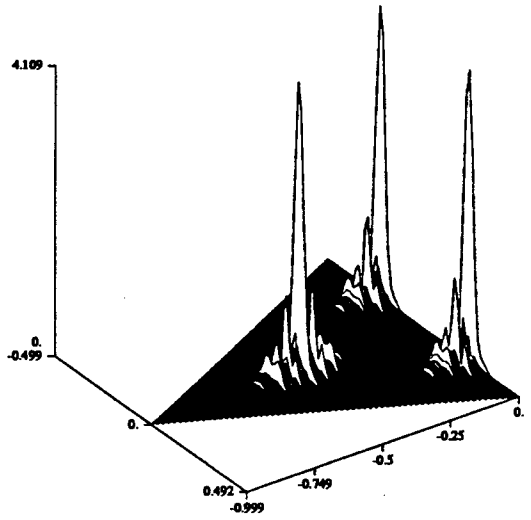

(a) A (N=1024, Np=64)

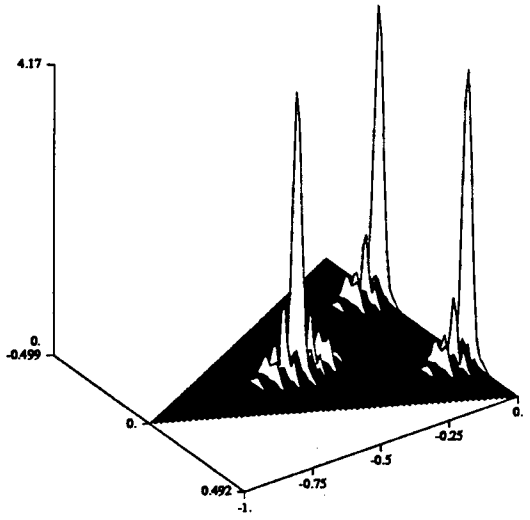

(b) A (N=4096, Np=64)

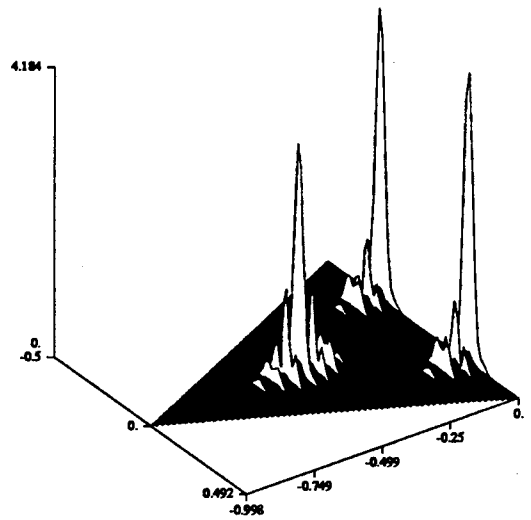

(c) A (N=16384, Np=64)

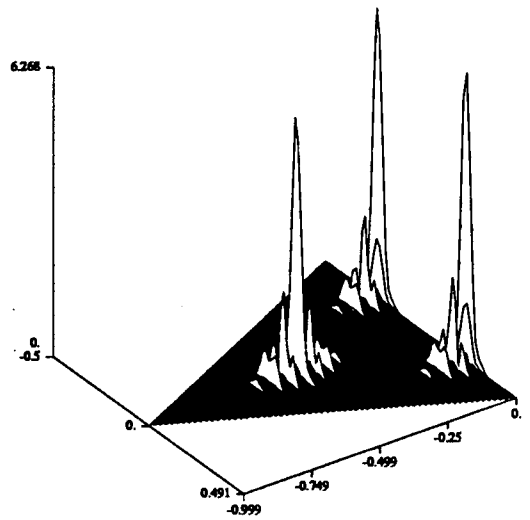

(d) A (N=32768, Np=64)

Figure 5: CS of a BPSK Signal: Varying the Observation Time.

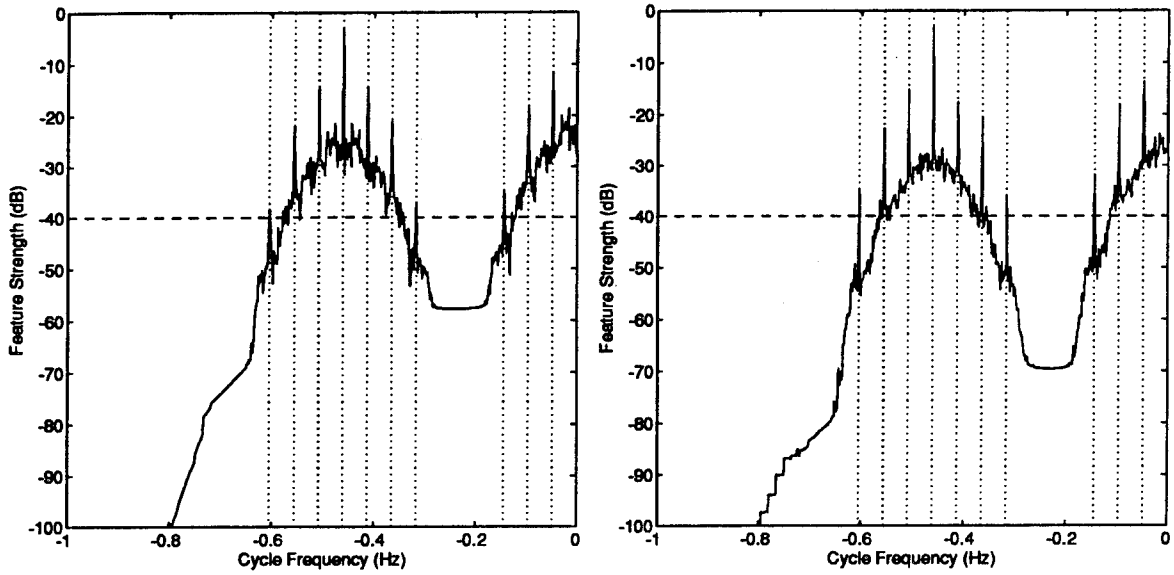

(a) A (N=1024,Np=64)

(b) A (N=4096, Np=64)

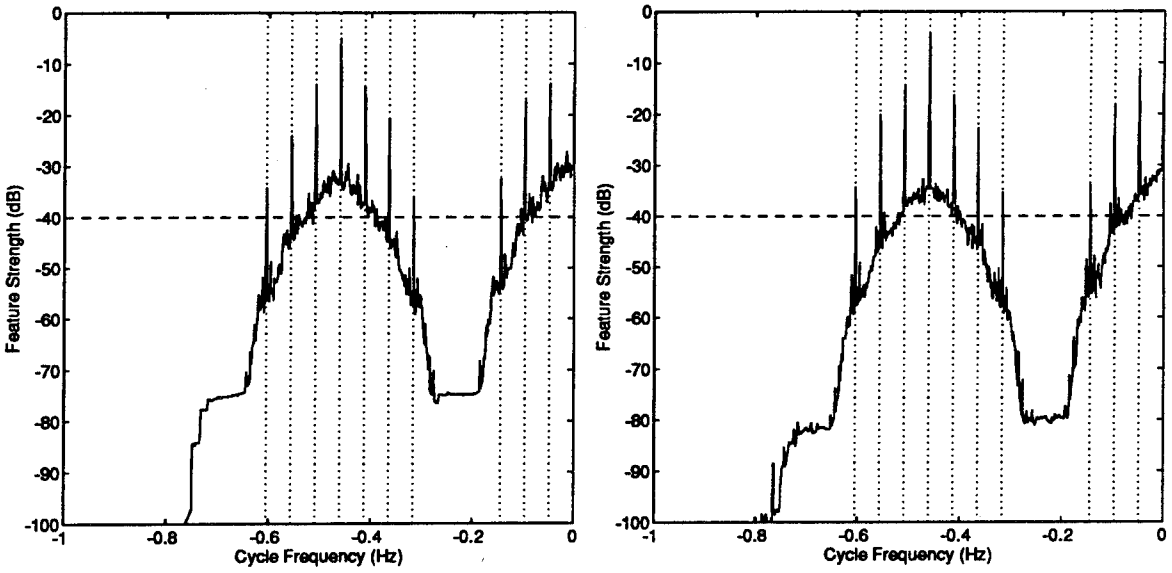

(c) A (N=16384, Np=64)

(d) A (N=32768, Np=64)

Figure 6: CFF of a BPSK Signal: Varying the Observation Time.

is used in order to more easily appreciate the distribution of cyclic spectral correlation components along the cycle frequencies. Each feature reveals itself as a discrete peak at a specific α corresponding to the theoretical value mentioned earlier for signal A. The measurement noise is visible on each graph and clearly decreases from (a) to (d) such that peaks exhibit higher SNR.

Next, the effect of varying the frequency resolution $\Delta f = 1/N_p$ on signal A is studied in Figure 7 and Figure 8. Using $\Delta f = \frac{1}{64}$, $\frac{1}{32}$, $\frac{1}{16}$, and $\frac{1}{8}$ in (a), (b), (c) and (d) respectively, a loss in frequency resolution appears in the CS (from (a) to (d)). On the other hand, the product $\Delta t \Delta f$ is increased. However, there should be some constraints imposed on Δf, i.e., for a BPSK signal having keying rate $1/T_A$,

$$\Delta f < \frac{1}{2T_A} \,. \tag{62}$$

In Figure 8(d), for example, $\Delta f = \frac{1}{8} = 0.125$ and $1/2T_A = 0.048/2 = 0.024$ and therefore $\Delta f > 1/2T_A$. As can be seen, this situation turns out to be undesirable since the baud rate feature decreases in strength and a highly distorted relationship between cyclic features arises.

Figure 9 to Figure 12 demonstrate the same varying parameters as for signal A but applied to a WGN signal N0. As observed, increasing the observation time without changing the frequency resolution reduces the noise measurement and its variance. As seen, the number of false detected features greatly reduces from (a) to (d). In general, the CFF inherently takes a specific shape such that the function clearly depicts a higher noise measurement variance as we approach $\alpha = \pm 1$ and the feature strengths decrease from (a) to (d). This particular shaping of the CFF is due to the region of support which was shown to be a diamond and therefore contains fewer points to rely on at the extremes. The effect of reducing the frequency resolution is studied in Figure 12. Due to the signals under investigations, N and N_p have been chosen to be 32768 and 64 respectively for all subsequent figures.

The CS and CFF of all noise-free BPSK signals are shown in Figure 13 and Figure 14 respectively. In (d), all signals have been combined and despite the fact that it is not possible to detect the 3 signals and their parameters by only analyzing the conventional PSD (at $\alpha = 0$), investigations of the CS or CFF reveal every signals'

peak to be considered. The dotted lines on the graphs appear on peaks which have been detected using a detection algorithm derived by the author. Quantitative results are provided in Appendix A.

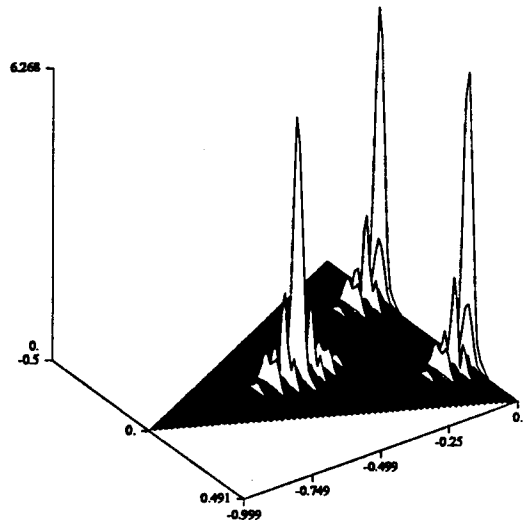

(a) A (N=32768,Np=64)

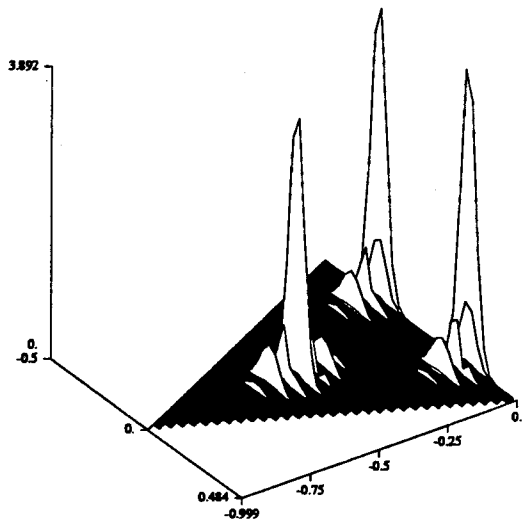

(b) A (N=32768, Np=32)

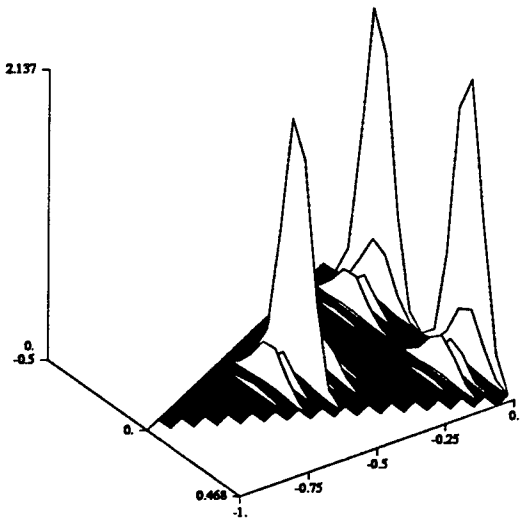

(c) A (N=32768, Np=16)

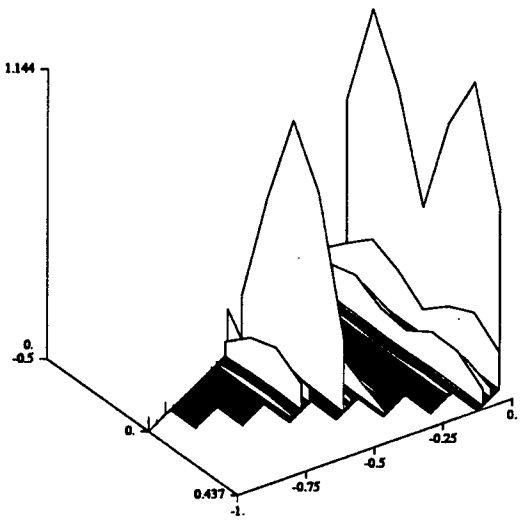

(d) A (N=32768, Np=8)

Figure 7: CS of a BPSK Signal: Varying the Frequency Resolution.

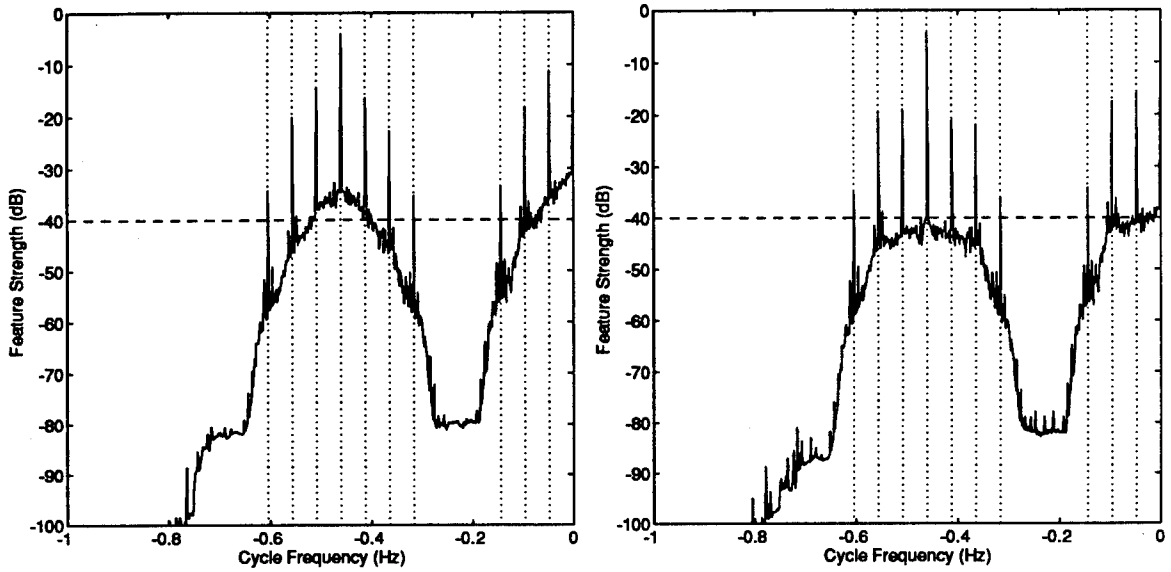

(a) A(N=32768,Np=64)

(b) A (N=32768, Np=32)

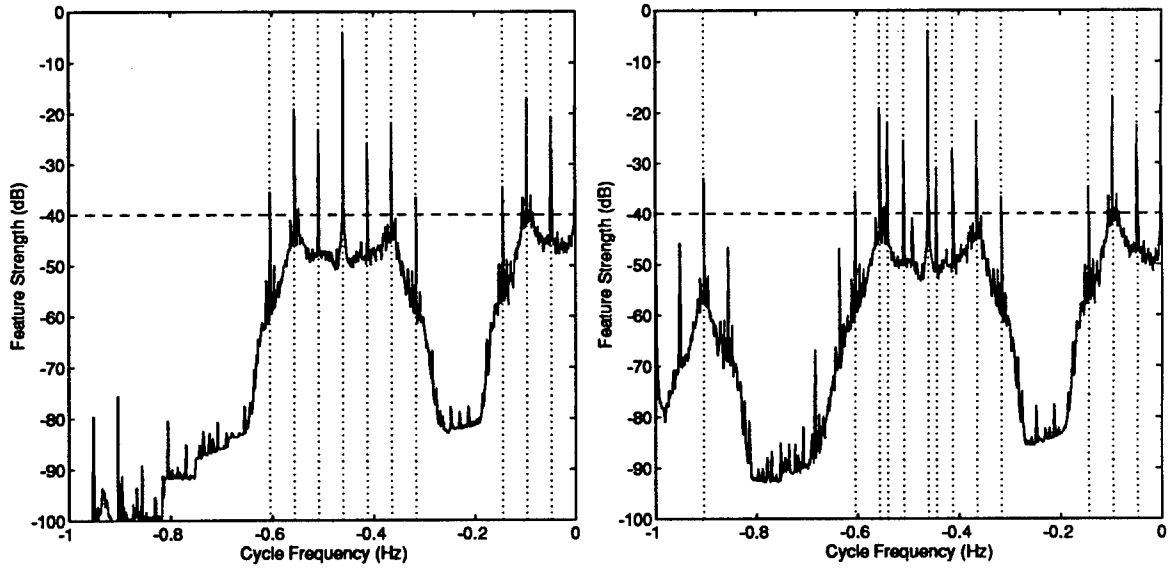

(c) A (N=32768, Np=16)

(d) A (N=32768, Np=8)

Figure 8: CFF of a BPSK Signal: Varying the Frequency Resolution.

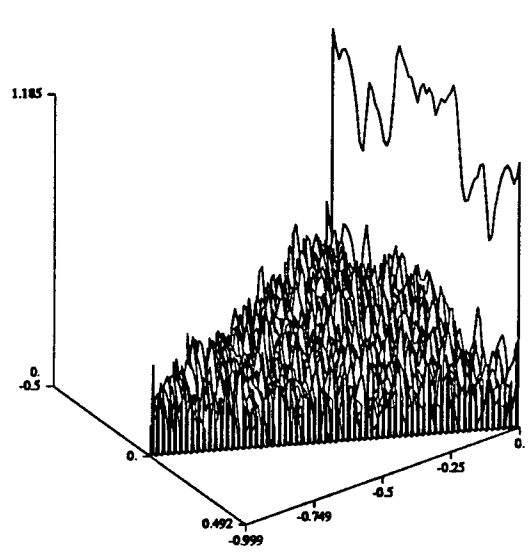

(a) N0 (N=1024, Np=64)

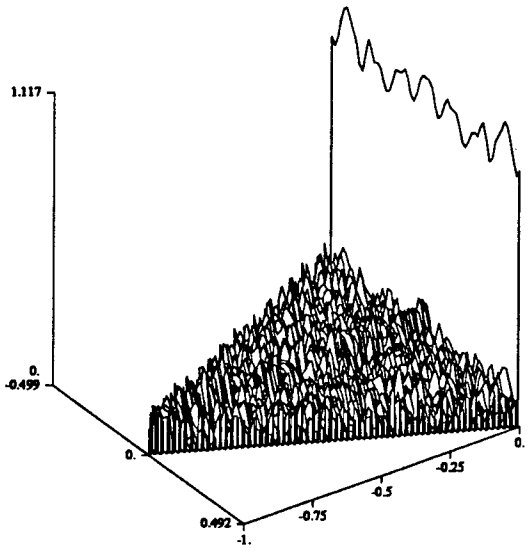

(b) N0 (N=4096, Np=64)

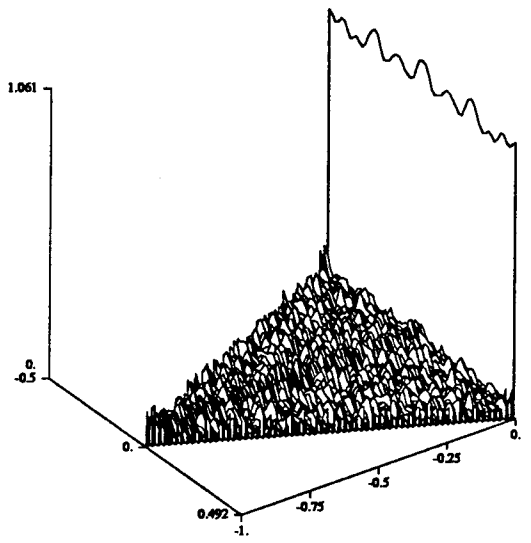

(c) N0 (N=16384, Np=64)

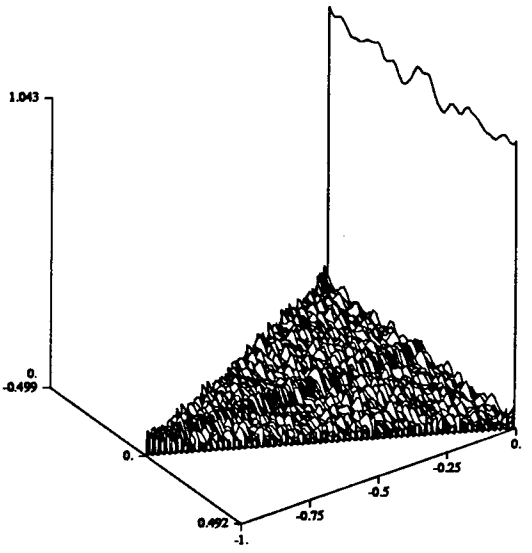

(d) N0 (N=32768, Np=64)

Figure 9: CS of Noise: Varying the Observation Time.

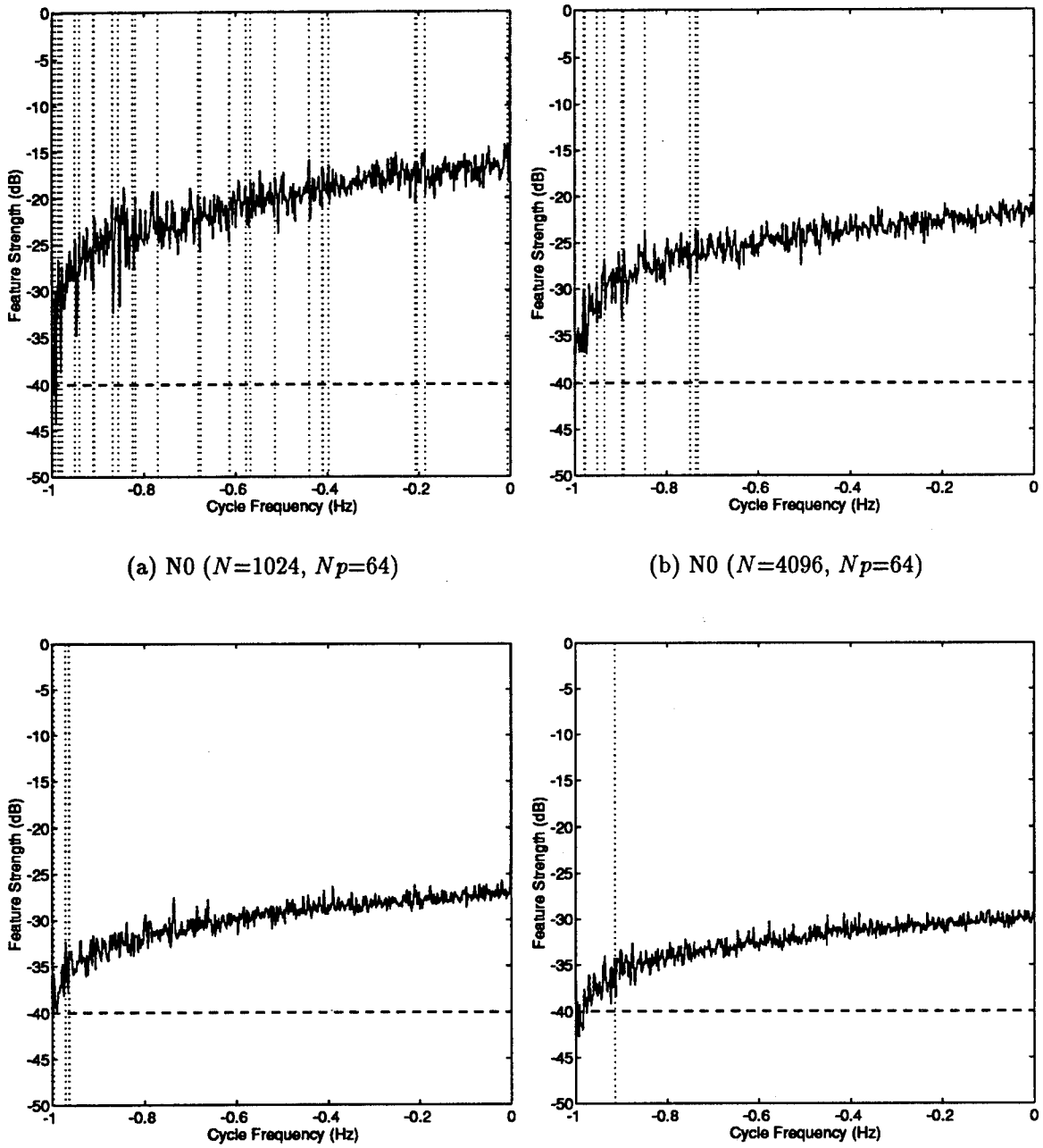

(a) N0 (N=1024, Np=64)

(b) N0 (N=4096, Np=64)

(c) N0 (N=16384, Np=64)

(d) N0 (N=32768, Np=64)

Figure 10: CFF of Noise: Varying the Observation Time.

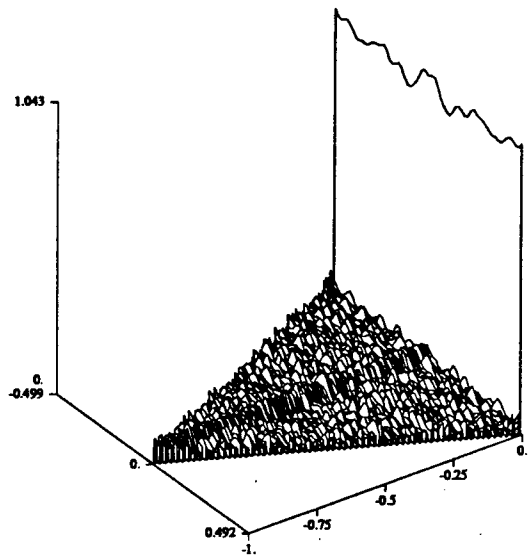

(a) N0 (N=32768, Np=64)

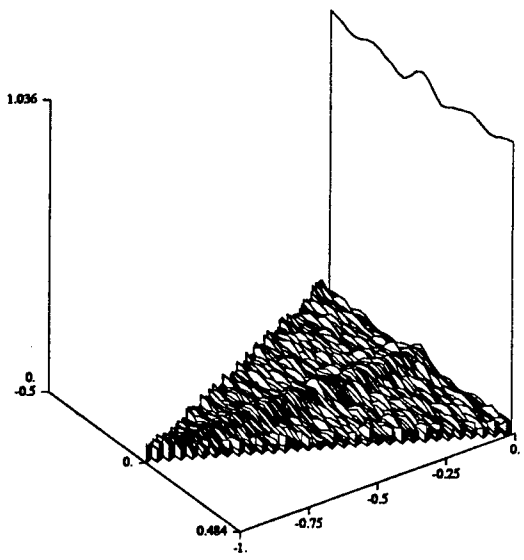

(b) N0 (N=32768, Np=32)

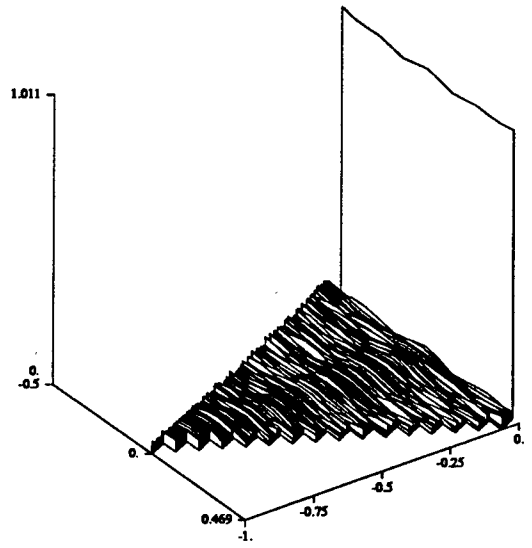

(c) N0 (N=32768, Np=16)

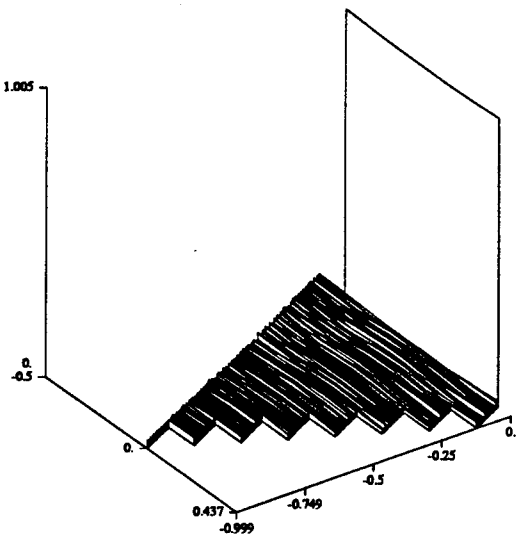

(d) N0 (N=32768, Np=8)

Figure 11: CS of Noise: Varying the Frequency Resolution.

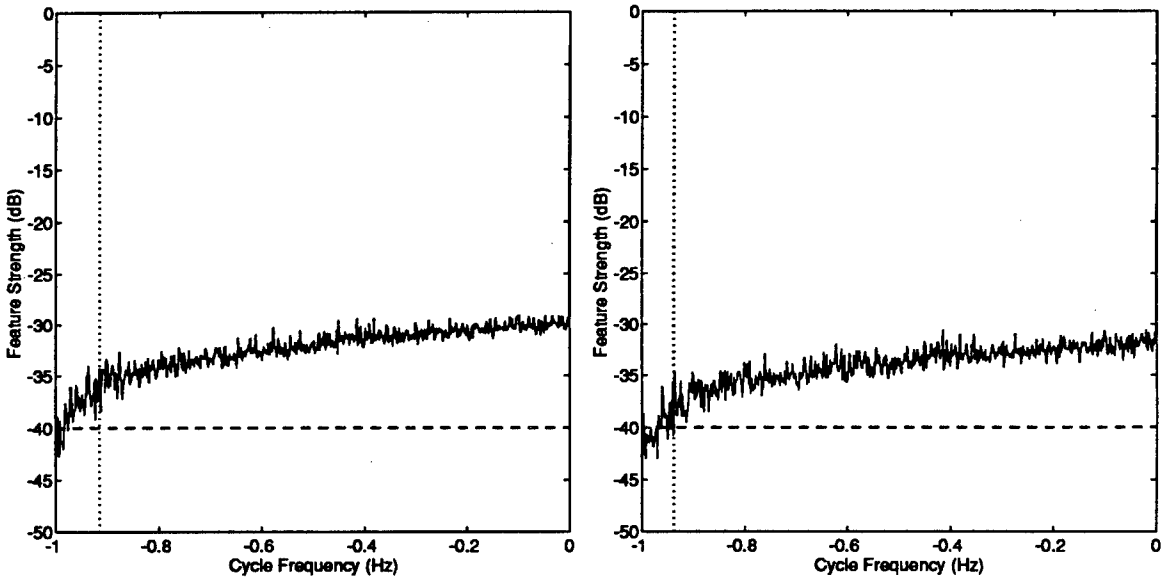

(a) N0 (N=32768, Np=64)

(b) N0 (N=32768, Np=32)

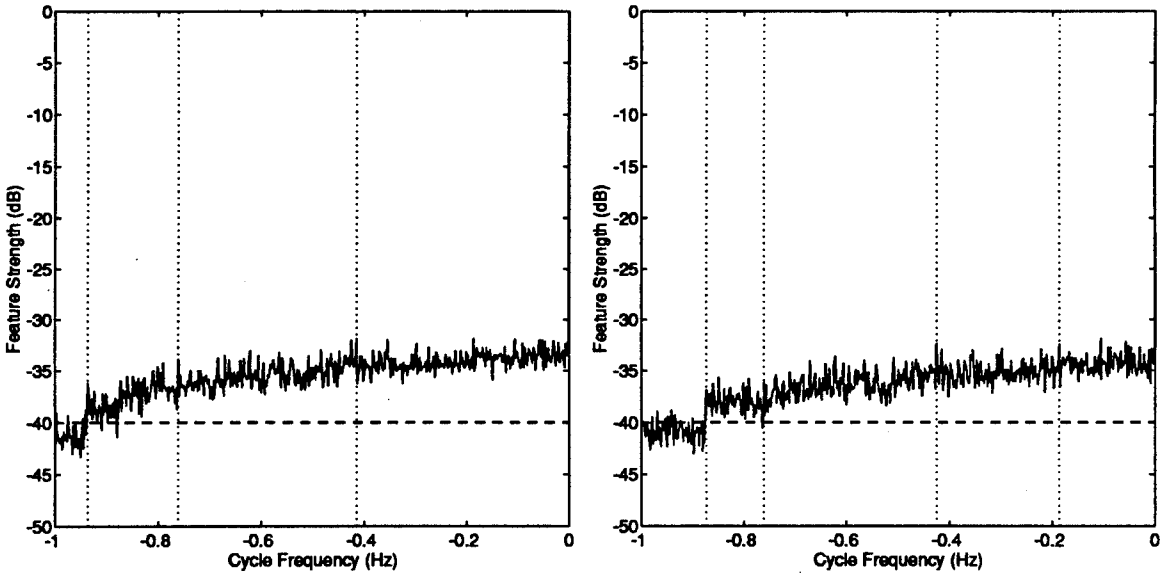

(c) N0 (N=32768, Np=16)

(d) N0 (N=32768, Np=8)

Figure 12: CFF of Noise: Varying the Frequency Resolution.

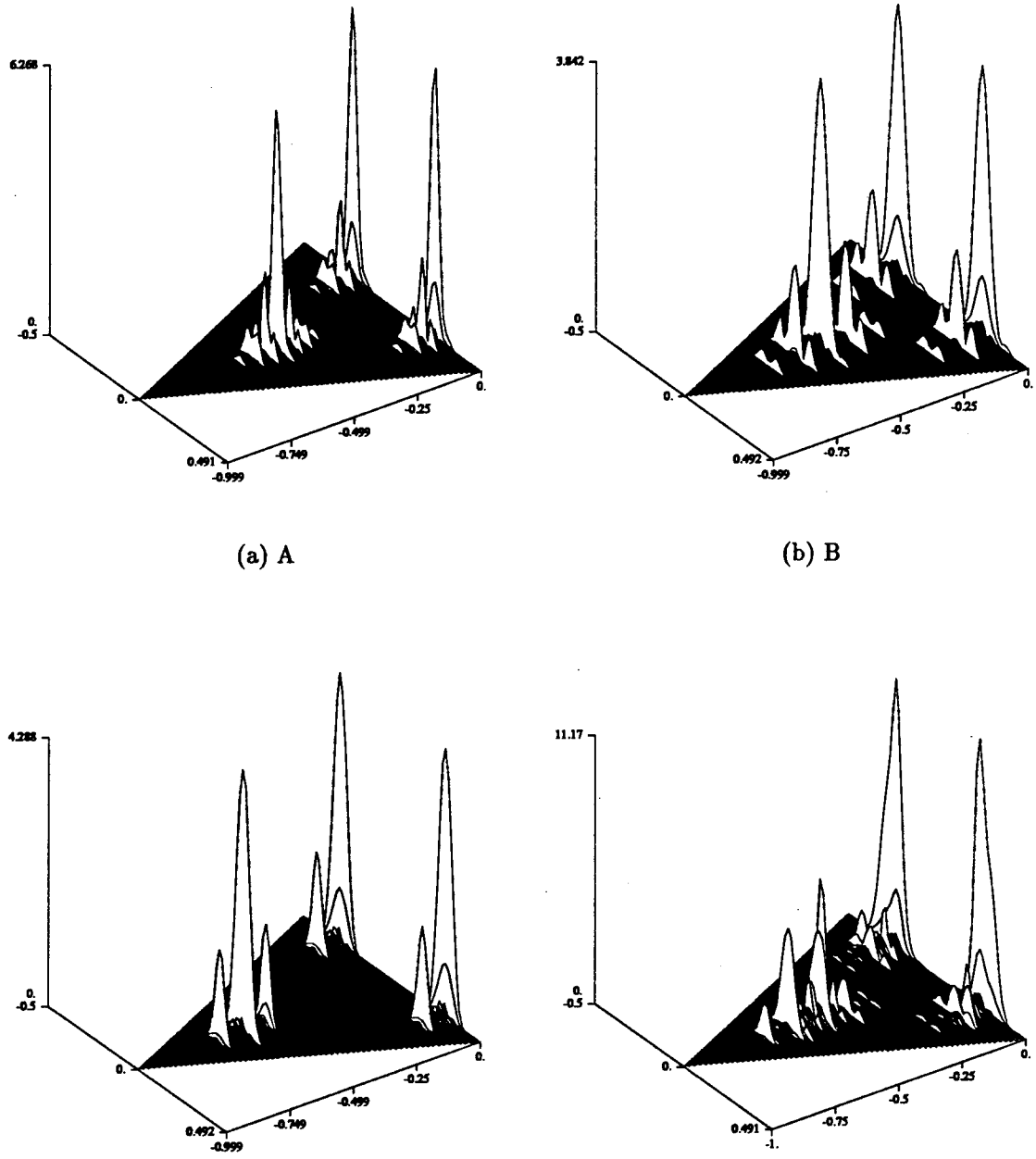

(a) A

(b) B

(c) C

(d) A+B+C

Figure 13: CS of Various BPSK Signals Using N=32768, Np=64.

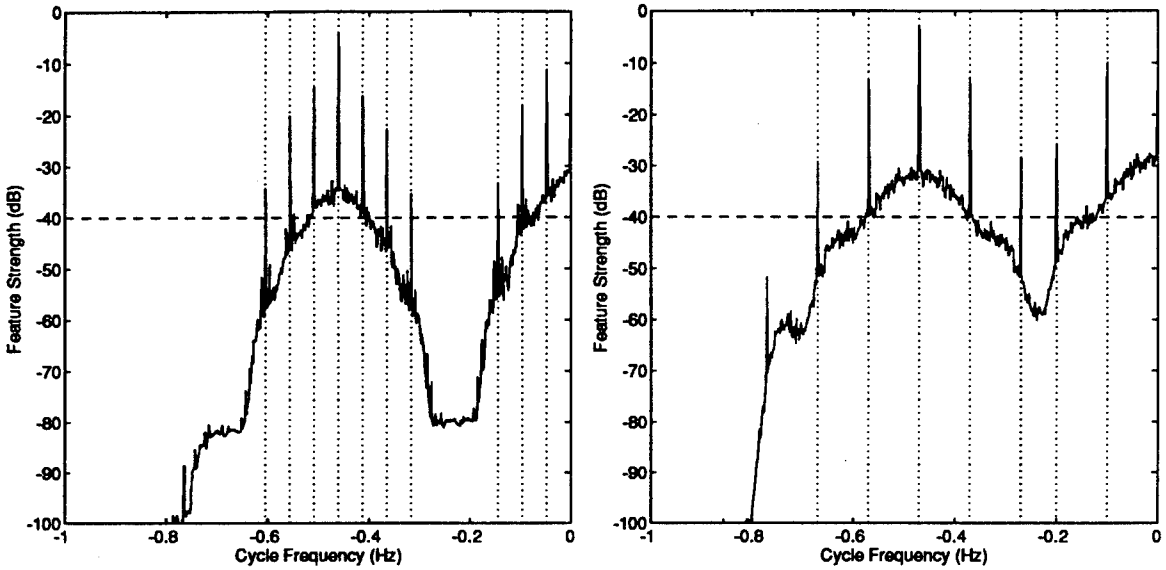

(a) A

(b) B

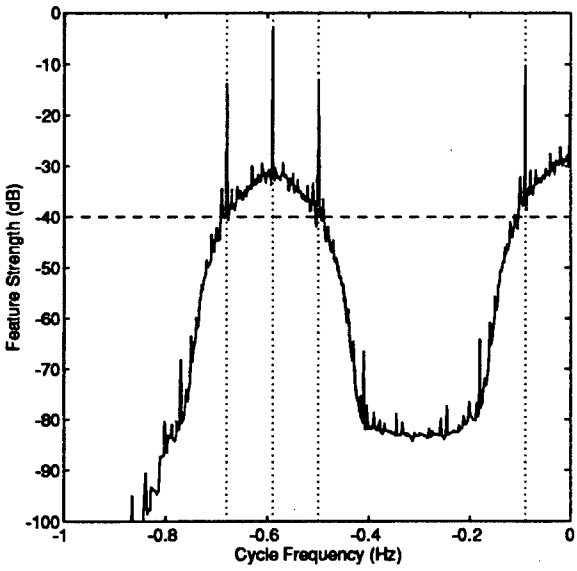

(c) C

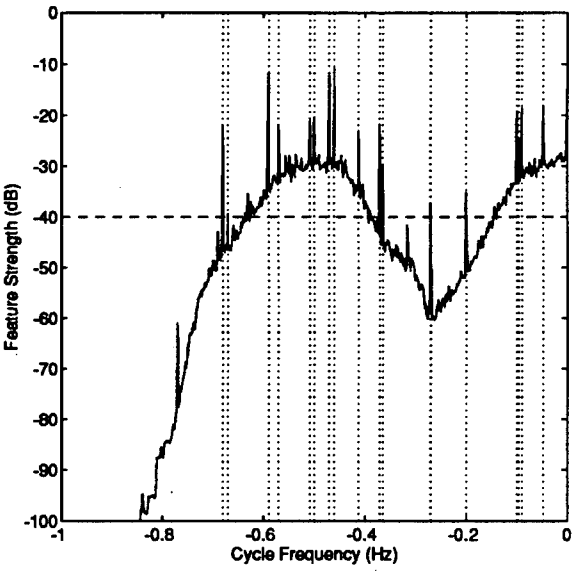

(d) A+B+C

Figure 14: CFF of Various BPSK Signals Using N=32768, Np=64.

parameters (see Table 10 of Appendix A). The effect of adding noise to these signals is studied from Figure 15 to Figure 18. Again, as the results tabulated in Appendix A quantify, all major features can still be detected. This undoubtly demonstrates the high degree of robustness and precision of the CS (or CFF) tools for analyzing cyclostationary communications signals.

4.4 SSCA Benchmarks on a SUN IPX

The computation time required for a SUN IPX to perform the SSCA using specific parameters are reported in Table 6 for reference. All timings are accurate to within 1 second and do not include the first and last steps of the algorithm which read the data, form the windows coefficients, and map and store the output. Note however that the time needed for these steps is relatively negligible.

Table 6: Results of SSCA Benchmarks on a SUN IPX.

N	N_p	$\Delta t \Delta f$	Time (sec)
1024	8	128	< 1
1024	16	64	1
1024	32	32	2
1024	64	16	4
4096	64	64	14
8192	64	128	30
16384	64	256	77
32768	64	512	169
32768	32	1024	81
32768	16	2048	41
32768	8	4096	20

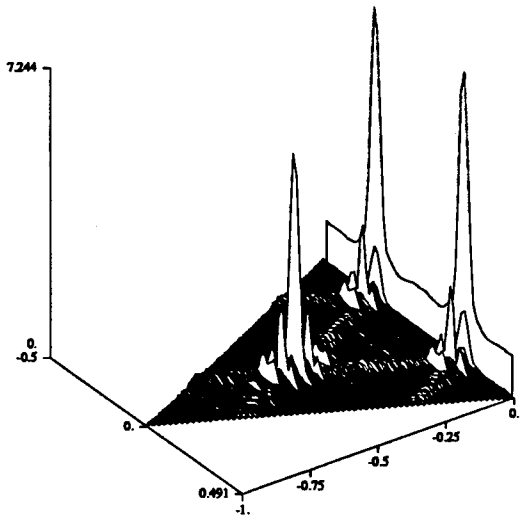

(a) A+N0

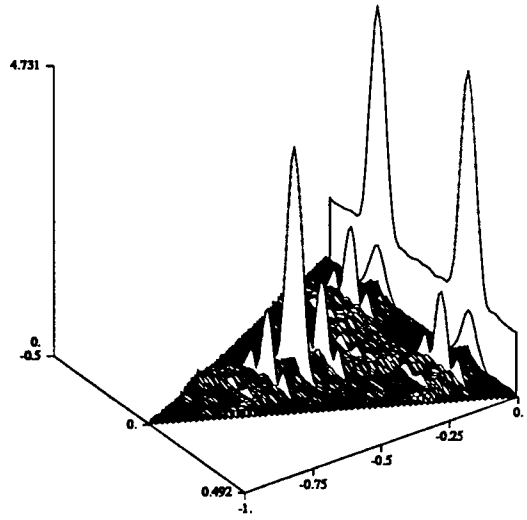

(b) B+N0

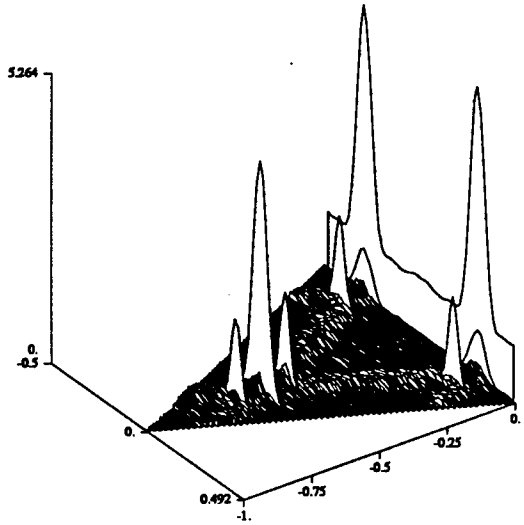

(c) C+N0

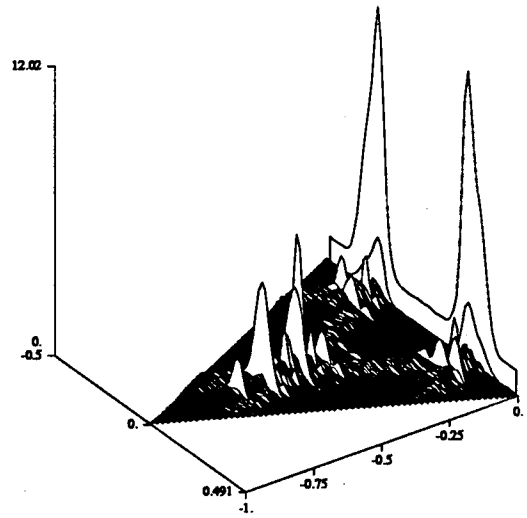

(d) A+B+C+N0

Figure 15: CS of Various BPSK Signals in Noise N0 Using N=32768, Np=64.

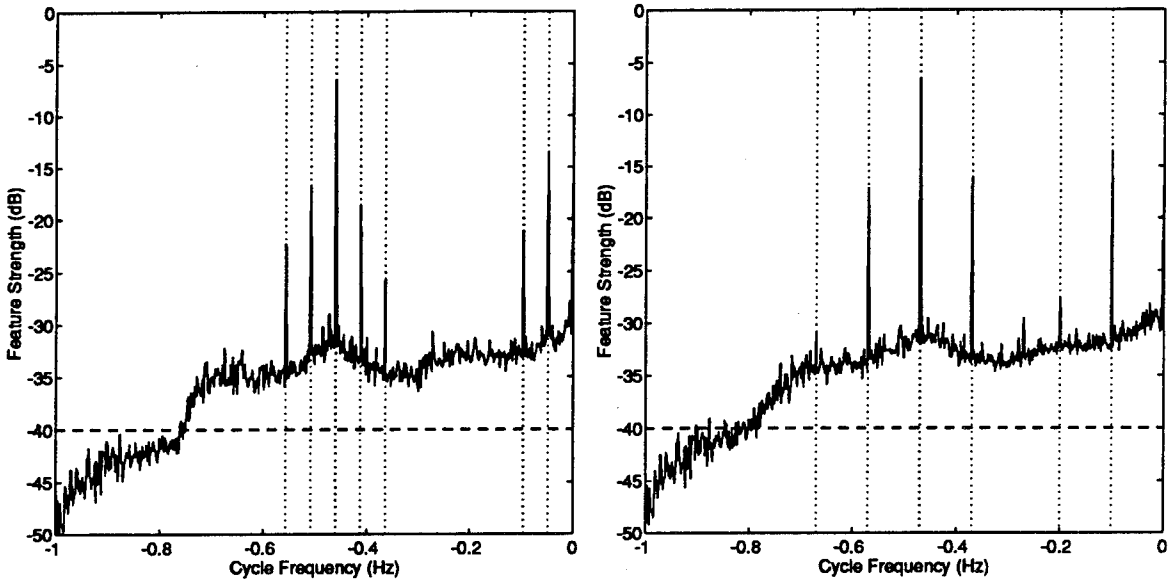

(a) A+N0

(b) B+N0

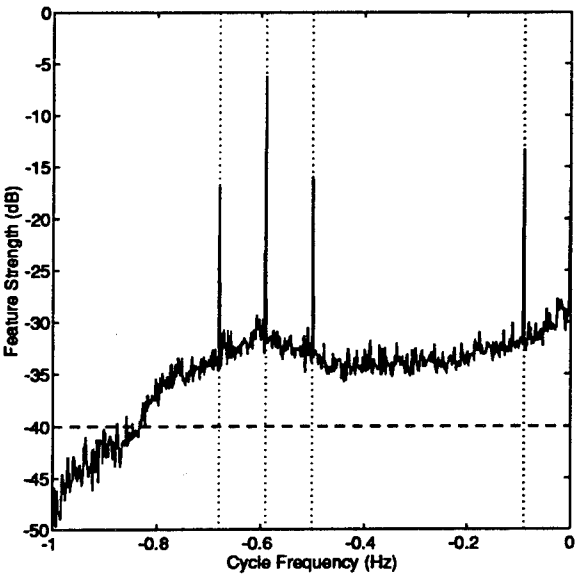

(c) C+N0

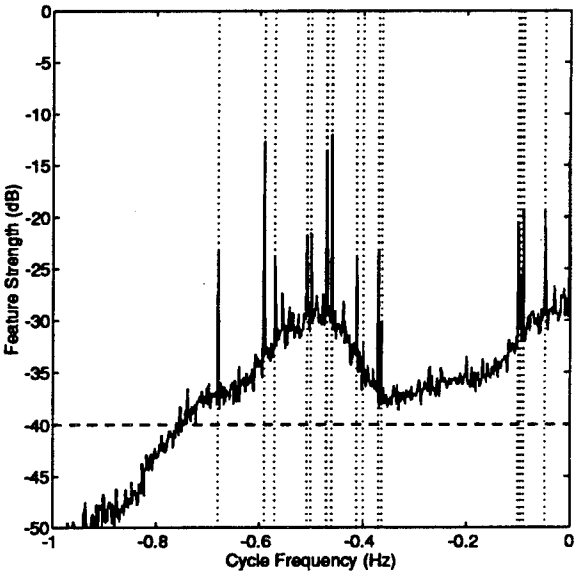

(d) A+B+C+N0

Figure 16: CFF of Various BPSK Signals in Noise N0 Using N=32768, Np=64.

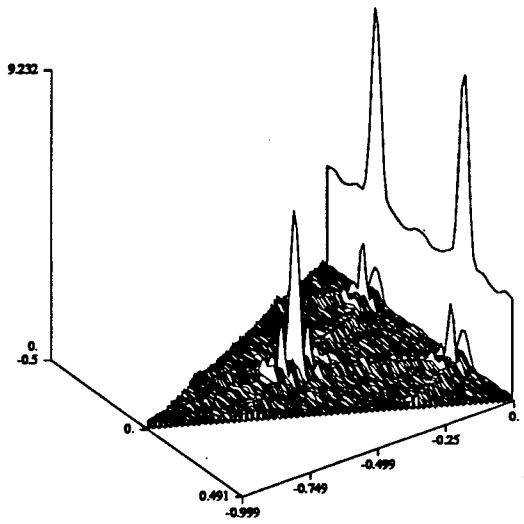

(a) A+N5

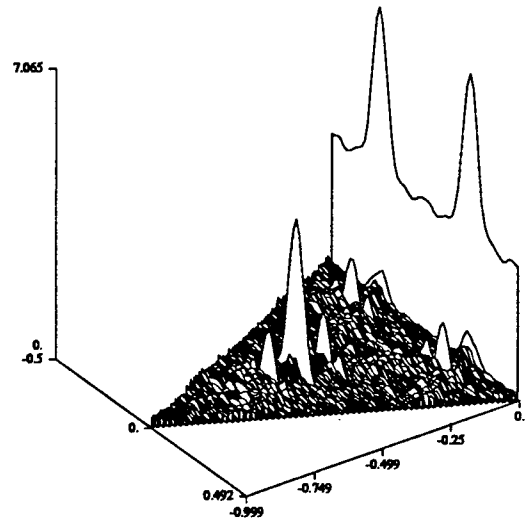

(b) B+N5

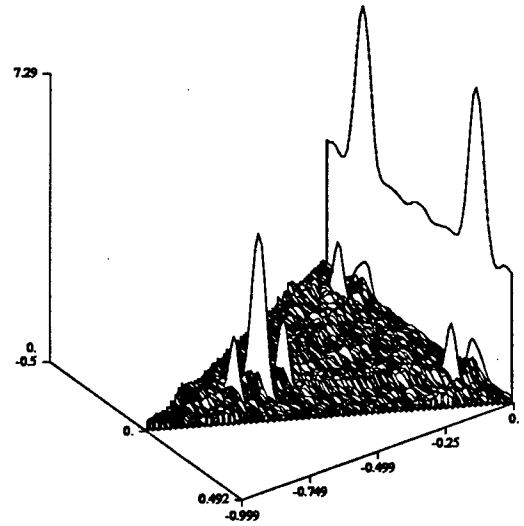

(c) C+N5

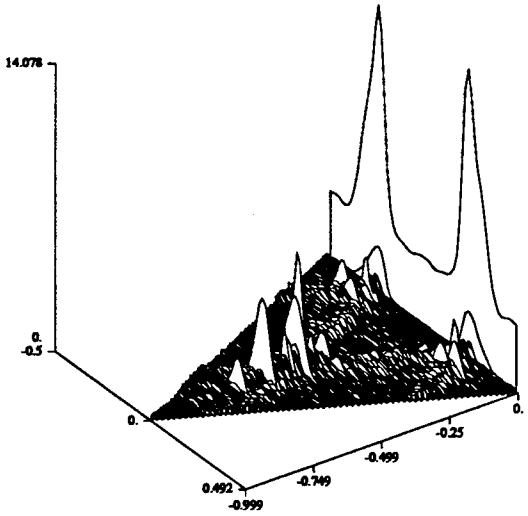

(d) A+B+C+N5

Figure 17: CS of Various BPSK Signals in Noise N5 Using N=32768, Np=64.

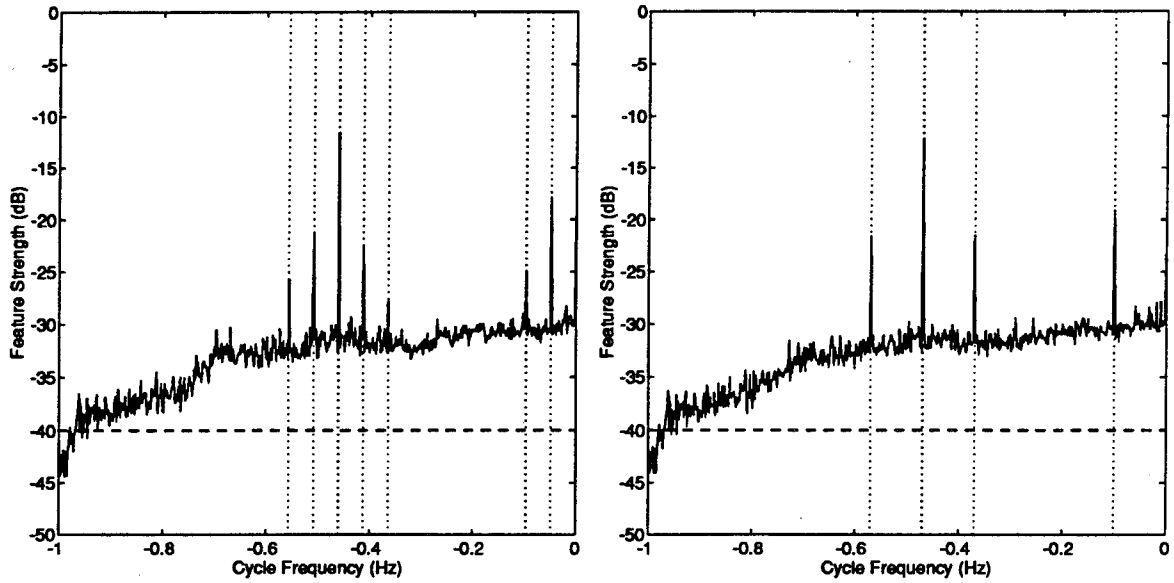

(a) A+N5

(b) B+N5

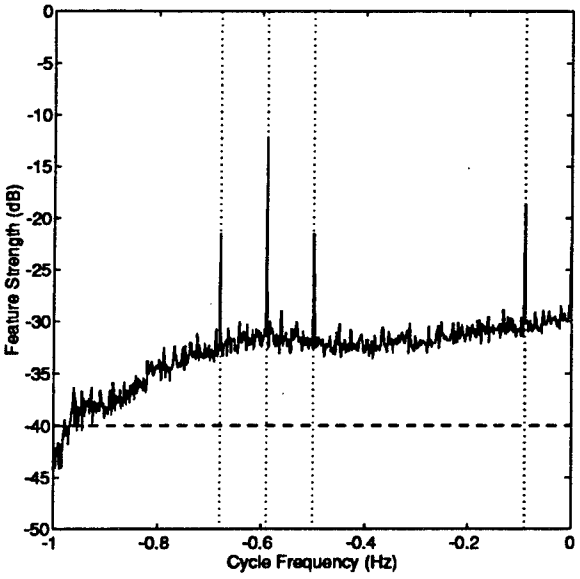

(c) C+N5

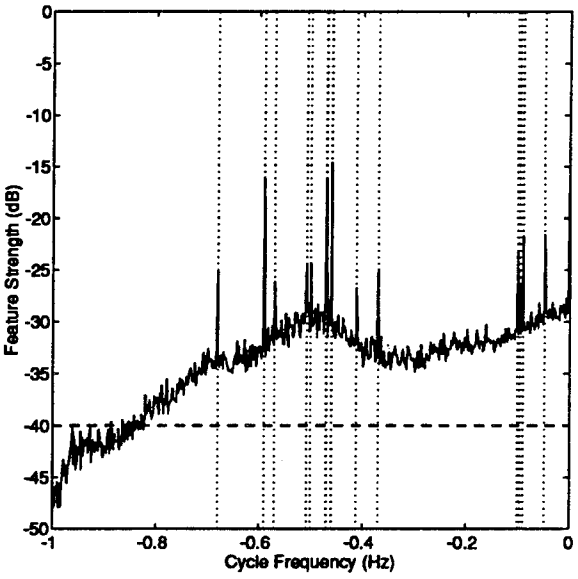

(d) A+B+C+N5

Figure 18: CFF of Various BPSK Signals in Noise N5 Using N=32768, Np=64.

5.0 SUMMARY AND CONCLUDING REMARKS

This report discussed the implementation of an efficient algorithm, the SSCA, for estimating the entire cyclic spectrum of discrete-time domain signals. Following a review on the theory of spectral correlation for cyclic spectral analysis of discrete-time signals, the SSCA was derived. The detailed description of the SSCA showed that it mainly reduces in complexity to a two-dimensional FFT of size $N \text{x} N_p$ and that it is suitable for parallel architectures. Parameters N and N_p specify a number of CS estimate attributes such as the frequency resolution Δf, the cycle frequency resolution $\Delta\alpha$, and the time-frequency resolution product $\Delta f \Delta t$. All the steps required to implement the SSCA were clearly explained. An analysis of the SSCA revealed its computational requirements. The accuracy of the estimates were also considered and an algorithm for mapping the SSCA output was provided. Additionally, the cyclic feature function (CFF) was defined as a means to detect the cyclic features from the SSCA.

Results of the SSCA encoded in C were then reported. Theoretical CSs were derived for three BPSK signals using various parameters and two additive white Gaussian noise (AWGN) signals. Plots of the CS and CFF of various combinations of these signals along with various algorithmic parameters were realized with the **ssca** program and presented to the reader. Specifically, the effect of varying the observation time and the frequency resolution were observed on one of the BPSK signal and one of the AWGN signal independently. Then, the CS and CFF of combinations of the signals under investigation were studied while all SSCA parameters were kept fixed. Cyclic features were detected based on the CFF. These experimental results show that all major cyclic features corresponding directly or indirectly to signal features (e.g. carrier frequency and baud rate in this case), were successfully detected even in highly corrupted conditions where conventional analysis would have failed to discriminate the signals. Finally, some benchmarks on the SUN for the SSCA were provided for reference.

In conclusion, the CS and CFF estimated with the SSCA have proven to be valuable tools for analyzing second-order cyclostationary communication signals and, by making extensive use of the FFT, to provide reliable and accurate results more efficiently than typical CS direct estimation methods. Based on these results, it is anticipated that the SSCA will be coded in a multi-C40 processors board in a near future and will be processing off-air data. Cyclic spectral analysis of live data composed of various modulation types signals will then be performed and the practical usefulness of the SSCA will be assessed.

APPENDIX

A.0 CYCLIC FEATURE DETECTION RESULTS

These results were found based on the Cyclic Feature Function (CFF) as defined in the main body of the report. A cyclic feature detection algorithm has been applied to the CFF producing tables of detected cyclic features. Each table shows the cyclic feature value α, its strength in dB, and to which signal feature it corresponds. The term FALSE means that the feature does not correlate with any signal's cyclic features. The detection algorithm used is not described here but is a fairly straightforward manner of detecting the features based on the CFF. Only results of the SSCA using $N = 32768$ and $N_p = 64$ are tabulated.

Table 7: A (N=32768, Np=64), 21 Features Detected.

α	Value (dB)	α	Value (dB)	Feature
0.00000	0.00			0
0.04800	-11.31	-0.04800	-11.31	f_{k_A}
0.09601	-18.17	-0.09601	-18.17	$2f_{k_A}$
0.14401	-33.48	-0.14401	-33.48	$3f_{k_A}$
0.31601	-35.39	-0.31601	-35.39	$2f_{c_A} - 3f_{k_A}$
0.36401	-22.83	-0.36401	-22.83	$2f_{c_A} - 2f_{k_A}$
0.41199	-16.43	-0.41199	-16.43	$2f_{c_A} - f_{k_A}$
0.45999	-4.08	-0.45999	-4.08	$2f_{c_A}$
0.50800	-14.34	-0.50800	-14.34	$2f_{c_A} + f_{k_A}$
0.55600	-20.17	-0.55600	-20.17	$2f_{c_A} + 2f_{k_A}$
0.60400	-34.42	-0.60400	-34.42	$2f_{c_A} + 3f_{k_A}$

APPENDIX

Table 8: B (N=32768, Np=64), 15 Features Detected.

α	Value (dB)	α	Value (dB)	Feature
0.00000	0.00			0
0.10001	-10.00	-0.10001	-10.00	f_{k_B}
0.20001	-25.80	-0.20001	-25.80	$2f_{k_B}$
0.26999	-28.36	-0.26999	-28.36	$2f_{c_B} - 3f_{k_B}$
0.37000	-12.81	-0.37000	-12.81	$2f_{c_B} - f_{k_B}$
0.47000	-3.03	-0.47000	-3.03	$2f_{c_B}$
0.57001	-13.26	-0.57001	-13.26	$2f_{c_B} + f_{k_B}$
0.67001	-29.30	-0.67001	-29.30	$2f_{c_B} + 2f_{k_B}$

Table 9: C (N=32768, Np=64), 9 Features Detected.

α	Value (dB)	α	Value (dB)	Feature
0.00000	0.00			0
0.09000	-10.24	-0.09000	-10.24	f_{k_C}
0.50000	-13.06	-0.50000	-13.06	$2f_{c_C} - f_{k_C}$
0.59000	-3.20	-0.59000	-3.20	$2f_{c_C}$
0.67999	-13.84	-0.67999	-13.84	$2f_{c_C} + f_{k_C}$

APPENDIX

Table 10: A+B+C (N=32768, Np=64), 35 Features Detected.

α	Value (dB)	α	Value (dB)	Feature
0.00000	0.00			0
0.04800	-18.15	-0.04800	-18.15	f_{k_A}
0.09000	-18.61	-0.09000	-18.61	f_{k_C}
0.09601	-24.83	-0.09601	-24.83	$2f_{k_A}$
0.10001	-19.25	-0.10001	-19.25	f_{k_B}
0.20001	-35.28	-0.20001	-35.28	$2f_{k_B}$
0.27000	-37.50	-0.27000	-37.50	$2f_{c_B} - 2f_{k_B}$
0.36401	-29.65	-0.36401	-29.65	$2f_{c_A} - 2f_{k_A}$
0.37000	-21.84	-0.37000	-21.84	$2f_{c_B} - f_{k_B}$
0.41199	-23.10	-0.41199	-23.10	$2f_{c_A} - f_{k_A}$
0.45999	-10.75	-0.45999	-10.75	$2f_{c_A}$
0.47000	-12.26	-0.47000	-12.26	$2f_{c_B}$
0.50000	-20.49	-0.50000	-20.49	$2f_{c_C} - f_{k_C}$
0.50800	-21.21	-0.50800	-21.21	$2f_{c_A} + f_{k_A}$
0.57001	-22.37	-0.57001	-22.37	$2f_{c_B} + f_{k_B}$
0.59000	-11.61	-0.59000	-11.61	$2f_{c_C}$
0.67001	-39.48	-0.67001	-39.48	$2f_{c_B} + 2f_{k_B}$
0.67999	-22.36	-0.67999	-22.36	$2f_{c_C} + f_{k_C}$

APPENDIX

Table 11: A+N0 (N=32768, Np=64), 15 Features Detected.

α	Value (dB)	α	Value (dB)	Feature
0.00000	0.00			0
0.04800	-13.53	-0.04800	-13.53	f_{k_A}
0.09601	-21.15	-0.09601	-21.15	$2f_{k_A}$
0.36401	-25.66	-0.36401	-25.66	$2f_{c_A} - 2f_{k_A}$
0.41199	-18.59	-0.41199	-18.59	$2f_{c_A} - f_{k_A}$
0.45999	-6.57	-0.45999	-6.57	$2f_{c_A}$
0.50800	-16.66	-0.50800	-16.66	$2f_{c_A} + f_{k_A}$
0.55600	-22.35	-0.55600	-22.35	$2f_{c_A} + 2f_{k_A}$

Table 12: B+N0 (N=32768, Np=64), 14 Features Detected.

α	Value (dB)	α	Value (dB)	Feature
0.00000	0.00			0
0.10001	-13.57	-0.10001	-13.57	f_{k_B}
0.20001	-27.66	-0.20001	-27.66	$2f_{k_B}$
0.37000	-16.05	-0.37000	-16.05	$2f_{c_B} - f_{k_B}$
0.47000	-6.69	-0.47000	-6.69	$2f_{c_B}$
0.57001	-17.10	-0.57001	-17.10	$2f_{c_B} + f_{k_B}$
0.66999	-30.82	-0.66999	-30.82	FALSE
0.73911	-34.07			FALSE

APPENDIX

Table 13: C+N0 (N=32768, Np=64), 9 Features Detected.

α	Value (dB)	α	Value (dB)	Feature
0.00000	0.00			0
0.09000	-13.33	-0.09000	-13.33	f_{kC}
0.50000	-15.96	-0.50000	-15.96	$2f_{cC} - f_{kC}$
0.59000	-6.27	-0.59000	-6.27	$2f_{cC}$
0.67999	-16.90	-0.67999	-16.90	$2f_{cC} + f_{kC}$

APPENDIX

Table 14: A+B+C+N0 (N=32768, Np=64), 31 Features Detected.

α	Value (dB)	α	Value (dB)	Feature
0.00000	0.00			0
0.04800	-19.28	-0.04800	-19.28	f_{k_A}
0.09000	-19.35	-0.09000	-19.35	f_{k_C}
0.09601	-25.77	-0.09601	-25.77	$2f_{k_A}$
0.10001	-20.54	-0.10001	-20.54	f_{k_B}
0.36401	-30.09	-0.36401	-30.09	$2f_{c_A} - 2f_{k_A}$
0.37000	-23.14	-0.37000	-23.14	$2f_{c_B} - f_{k_B}$
0.39948	-32.17	-0.39948	-32.17	FALSE
0.41199	-23.80	-0.41199	-23.80	$2f_{c_A} - f_{k_A}$
0.45999	-12.02	-0.45999	-12.02	$2f_{c_A}$
0.47000	-13.75	-0.47000	-13.75	$2f_{c_B}$
0.50000	-21.61	-0.50000	-21.61	$2f_{c_C} - f_{k_C}$
0.50800	-21.79	-0.50800	-21.79	$2f_{c_A} + f_{k_A}$
0.57001	-23.99	-0.57001	-23.99	$2f_{c_B} + f_{k_B}$
0.59000	-12.70	-0.59000	-12.70	$2f_{c_C}$
0.67999	-23.34	-0.67999	-23.34	$2f_{c_C} + f_{k_C}$

APPENDIX

Table 15: A+N5 (N=32768, Np=64), 15 Features Detected.

α	Value (dB)	α	Value (dB)	Feature
0.00000	0.00			0
0.04800	-17.87	-0.04800	-17.87	f_{k_A}
0.09601	-24.95	-0.09601	-24.95	$2f_{k_A}$
0.36401	-27.89	-0.36401	-27.89	$2f_{c_A} - 2f_{k_A}$
0.41199	-22.47	-0.41199	-22.47	$2f_{c_A} - f_{k_A}$
0.45999	-11.54	-0.45999	-11.54	$2f_{c_A}$
0.50800	-21.32	-0.50800	-21.32	$2f_{c_A} + f_{k_A}$
0.55600	-25.68	-0.55600	-25.68	$2f_{c_A} + 2f_{k_A}$

Table 16: B+N5 (N=32768, Np=64), 9 Features Detected.

α	Value (dB)	α	Value (dB)	Feature
0.00000	0.00			0
0.10001	-19.07	-0.10001	-19.07	f_{k_B}
0.37000	-21.53	-0.37000	-21.53	$2f_{c_B} - f_{k_B}$
0.47000	-12.15	-0.47000	-12.15	$2f_{c_B}$
0.57001	-21.65	-0.57001	-21.65	$2f_{c_B} + f_{k_B}$

APPENDIX

Table 17: C+N5 (N=32768, Np=64), 9 Features Detected.

α	Value (dB)	α	Value (dB)	Feature
0.00000	0.00			0
0.09000	-18.75	-0.09000	-18.75	f_{k_C}
0.50000	-21.52	-0.50000	-21.52	$2f_{c_C} - f_{k_C}$
0.59000	-12.17	-0.59000	-12.17	$2f_{c_C}$
0.67999	-21.54	-0.67999	-21.54	$2f_{c_C} + f_{k_C}$

Table 18: A+B+C+N5 (N=32768, Np=64), 27 Features Detected.

α	Value (dB)	α	Value (dB)	Feature
0.00000	0.00			0
0.04800	-21.62	-0.04800	-21.62	f_{k_A}
0.09000	-21.70	-0.09000	-21.70	f_{k_C}
0.09601	-26.59	-0.09601	-26.59	$2f_{k_A}$
0.10001	-23.22	-0.10001	-23.22	f_{k_B}
0.37000	-24.94	-0.37000	-24.94	$2f_{c_B} - f_{k_B}$
0.41199	-26.79	-0.41199	-26.79	$2f_{c_A} - f_{k_A}$
0.45999	-14.57	-0.45999	-14.57	$2f_{c_A}$
0.47000	-16.26	-0.47000	-16.26	$2f_{c_B}$
0.50000	-24.36	-0.50000	-24.36	$2f_{c_C} - f_{k_C}$
0.50800	-24.55	-0.50800	-24.55	$2f_{c_A} + f_{k_A}$
0.57001	-26.13	-0.57001	-26.13	$2f_{c_B} + f_{k_B}$
0.59000	-16.03	-0.59000	-16.03	$2f_{c_C}$
0.67999	-25.18	-0.67999	-25.18	$2f_{c_C} + f_{k_C}$

REFERENCES

[1] W. A. Gardner, "Signal Interception: A Unifying Theoretical Framework for Feature Detection," IEEE Transactions on Communications, vol. COM-36, pp. 897–906, August 1988.

[2] W. A. Gardner, "Exploitation of Spectral Redundancy in Cyclostationary Signals," IEEE Signal Processing Magazine, pp. 4–35, April 1991.

[3] R. S. Roberts, W. A. Brown and H. H. Loomis, Jr., "Computationally Efficient Algorithms for Cyclic Spectral Analysis," IEEE Signal Processing Magazine, pp. 38–49, April 1991.

[4] R. S. Roberts, Architectures for Digital Cyclic Spectral Analysis. PhD thesis, University of California, Davis, CA, September 1989.

[5] W. A. Gardner, Introduction to Random Processes with Applications to Signals and Systems. New York: Second Edition, McGraw-Hill, 1990.

[6] W. A. Gardner, Statistical Spectral Analysis: A Non-probabilistic Theory. Englewood Cliffs, NJ: Prentice-Hall, 1987.

[7] W. A. Brown, On the Theory of Cyclostationary Signals. PhD thesis, University of California, Davis, CA, September 1987.

[8] W. A. Brown and H. H. Loomis, Jr., "Digital Implementations of Spectral Correlation Analyzers," in Proceedings of the Fourth Annual ASSP Workshop on Spectrum Estimation and modeling, (Minneapolis, Mn), pp. 264–270, August 1988.

[9] W. A. Brown and H. H. Loomis, Jr., "Digital Implementations of Spectral Correlation Analyzers," IEEE Transactions on Signal Processing, vol. 41, pp. 703–720, February 1993.

[10] G. D. Zivanovic and W. A. Gardner, "Degrees of Cyclostationarity and Their Applications to Signal Detection and Estimation," Signal Processing, vol. 22, pp. 287–297, April 1991.

[11] C.-K. Chen, Spectral Correlation Characterization of Modulated Signals with Applications to Signal Detection and Source Location. PhD thesis, University of California, Davis, CA, 1989.

DOCUMENT CONTROL DATA

(Security classification of title, body of abstract and indexing annotation must be entered when the overall document is classified)

1. ORIGINATOR (the name and address of the organization preparing the document. Organizations for whom the document was prepared, e.g. Establishment sponsoring a contractor's report, or tasking agency, are entered in section 8.)

DEFENCE RESEARCH ESTABLISHMENT OTTAWA
NATIONAL DEFENCE
SHIRLEYS BAY, OTTAWA, ONTARIO K1A 0K2 CANADA

2. SECURITY CLASSIFICATION (overall security classification of the document. including special warning terms if applicable)

UNCLASSIFIED

3. TITLE (the complete document title as indicated on the title page. Its classification should be indicated by the appropriate abbreviation (S,C or U) in parentheses after the title.)

ON THE IMPLEMENTATION OF THE STRIP SPECTRAL CORRELATION ALGORITHM FOR CYCLIC SPECTRUM ESTIMATION (U)

4. AUTHORS (Last name, first name, middle initial)

APRIL, ERIC

5. DATE OF PUBLICATION (month and year of publication of document)

MARCH 1994

6a. NO. OF PAGES (total containing information. Include Annexes, Appendices, etc.)

51

6b. NO. OF REFS (total cited in document)

11

7. DESCRIPTIVE NOTES (the category of the document, e.g. technical report, technical note or memorandum. If appropriate, enter the type of report, e.g. interim, progress, summary, annual or final. Give the inclusive dates when a specific reporting period is covered.)

DREO TECHNICAL NOTE

8. SPONSORING ACTIVITY (the name of the department project office or laboratory sponsoring the research and development. Include the address.)

DEFENCE RESEARCH ESTABLISHMENT OTTAWA
NATIONAL DEFENCE
SHIRLEYS BAY, OTTAWA, ONTARIO K1A 0K2 CANADA

9a. PROJECT OR GRANT NO. (if appropriate, the applicable research and development project or grant number under which the document was written. Please specify whether project or grant)

041LK11

9b. CONTRACT NO. (if appropriate, the applicable number under which the document was written)

10a. ORIGINATOR'S DOCUMENT NUMBER (the official document number by which the document is identified by the originating activity. This number must be unique to this document.)

DREO TECHNICAL NOTE 94-2

10b. OTHER DOCUMENT NOS. (Any other numbers which may be assigned this document either by the originator or by the sponsor)

11. DOCUMENT AVAILABILITY (any limitations on further dissemination of the document, other than those imposed by security classification)

XX) Unlimited distribution
( ) Distribution limited to defence departments and defence contractors; further distribution only as approved
( ) Distribution limited to defence departments and Canadian defence contractors; further distribution only as approved
( ) Distribution limited to government departments and agencies; further distribution only as approved
( ) Distribution limited to defence departments; further distribution only as approved
( ) Other (please specify):

12. DOCUMENT ANNOUNCEMENT (any limitation to the bibliographic announcement of this document. This will normally correspond to the Document Availabilty (11). However, where further distribution (beyond the audience specified in 11) is possible, a wider announcement audience may be selected.)

UNCLASSIFIED

SECURITY CLASSIFICATION OF FORM

13. ABSTRACT (a brief and factual summary of the document. It may also appear elsewhere in the body of the document itself. It is highly desirable that the abstract of classified documents be unclassified. Each paragraph of the abstract shall begin with an indication of the security classification of the information in the paragraph (unless the document itself is unclassified) represented as (S), (C), or (U). It is not necessary to include here abstracts in both offical languages unless the text is bilingual).

(U) This report discusses the implementation of one of the best digital cyclic spectrum (CS) algorithms derived so far, the Strip Spectral Correlation Algorithm (SSCA). Some theoretical background and a detailed description of the SSCA are provided. An analysis of the SSCA is performed and an algorithm for mapping the SSCA output is formulated. The cyclic feature function (CFF) is defined as a means to detect the cyclic features from the SSCA. Results of the SSCA encoded in C are then reported. Three BPSK signals and two additive white Gaussian noise (AWGN) signals are used to verify the validity of the SSCA. Three-dimensional plots and two-dimensional plots of the CS and CFF respectively are presented to the reader. Finally, some benchmarks on a SUN computer for the SSCA are provided for reference. In brief, the CS and CFF estimated with the SSCA prove to be valuable tools for analyzing second-order cyclostationary communication signals and, by making extensive use of the FFT, to provide robust, reliable, and accurate results more efficiently than typical CS direct estimation methods.

14. KEYWORDS, DESCRIPTORS or IDENTIFIERS (technically meaningful terms or short phrases that characterize a document and could be helpful in cataloguing the document. They should be selected so that no security classification is required. Identifiers, such as equipment model designation, trade name, military project code name, geographic location may also be included. If possible keywords should be selected from a published thesaurus. e.g. Thesaurus of Engineering and Scientific Terms (TEST) and that thesaurus-identified. If it is not possible to select indexing terms which are Unclassified, the classification of each should be indicated as with the title.)

CYCLOSTATIONARY
SIGNAL PROCESSING
SPECTRAL ESTIMATION
CYCLIC FEATURE
SPECTRAL CORRELATION
SIGNAL DETECTION